

NASA TECHNICAL
MEMORANDUM

NASA TM X-53760

1048

NASA TM X-53760

GPO PRICE \$ _____

CFSTI PRICE(S) \$ _____

Hard copy (HC) _____

Microfiche (MF) _____

ff 653 July 65

AIRBORNE INSTRUMENTATION AND DATA TRANSMISSION
RESEARCH AT MSFC

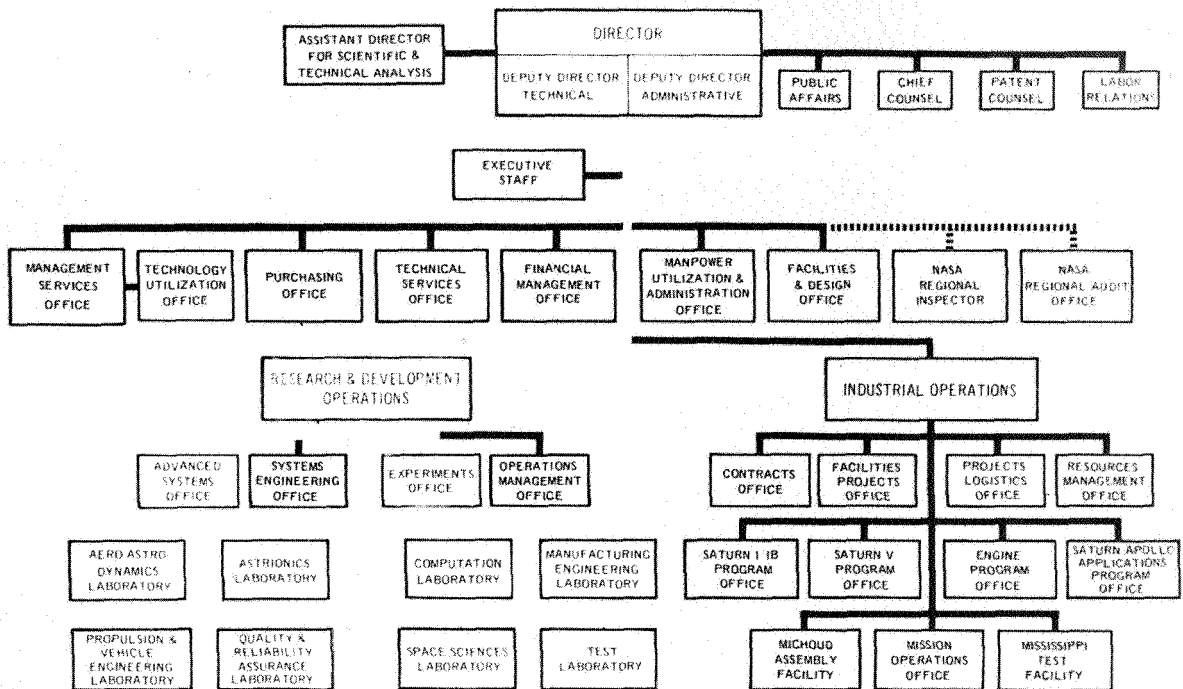
RESEARCH ACHIEVEMENTS REVIEW
VOLUME III REPORT NO. 1

RESEARCH AND DEVELOPMENT OPERATIONS
GEORGE C. MARSHALL SPACE FLIGHT CENTER
MARSHALL SPACE FLIGHT CENTER, ALABAMA



FACILITY FORM 602	N 68-38161	
	(ACCESSION NUMBER)	(THRU)
	57 (PAGES)	1 (CODE)
	TMX 53760 (NASA CR OR TMX OR AD NUMBER)	07 (CATEGORY)

GEORGE C. MARSHALL SPACE FLIGHT CENTER



RESEARCH ACHIEVEMENTS REVIEWS COVER THE FOLLOWING FIELDS OF RESEARCH

- Radiation Physics
- Thermophysics
- Chemical Propulsion
- Cryogenic Technology
- Electronics
- Control Systems
- Materials
- Manufacturing
- Ground Testing
- Quality Assurance and Checkout
- Terrestrial and Space Environment
- Aerodynamics
- Instrumentation
- Power Systems
- Guidance Concepts
- Astrodynamics
- Advanced Tracking Systems
- Communication Systems
- Structures
- Mathematics and Computation
- Advanced Propulsion
- Lunar and Meteoroid Physics

NATIONAL AERONAUTICS AND SPACE ADMINISTRATION
WASHINGTON, D.C.

RESEARCH ACHIEVEMENTS REVIEW
VOLUME III **REPORT NO. 1**

Rept. 1

AIRBORNE INSTRUMENTATION AND DATA TRANSMISSION
RESEARCH AT MSFC

RESEARCH AND DEVELOPMENT OPERATIONS
GEORGE C. MARSHALL SPACE FLIGHT CENTER
MARSHALL SPACE FLIGHT CENTER, ALABAMA

PRECEDING PAGE BLANK NOT FILMED.

~~KALC~~

PREFACE

In February, 1965, Dr. Ernst Stuhlinger, Director, Research Projects Laboratory (now Space Sciences Laboratory), initiated a series of Research Achievements Reviews which set forth those achievements accomplished by the laboratories of the Marshall Space Flight Center. Each review covered one or two fields of research in a form readily usable by specialists, systems engineers and program managers. The review of February 24, 1966, completed this series. Each review was documented in the "Research Achievements Review Series."

In March, 1966, a second series of Research Achievements Reviews was initiated. This second series emphasized research areas of greatest concentration of effort, of most rapid progress, or of most pertinent interest and was published as "Research Achievements Review Reports, Volume II." Volume II covered the reviews from March, 1966, through February, 1968.

This third series of Research Achievements Reviews was begun in March, 1968, and continues the concept introduced in the second series. Reviews of the third series are designated Volume III and will span the period from March, 1968, through February, 1970.

The papers in this report were presented March 28, 1968.

William G. Johnson
Director
Experiments Office

PRECEDING PAGE BLANK NOT FILMED.

CONTENTS . . .

	Page
INTRODUCTION TO AIRBORNE INSTRUMENTATION AND DATA TRANSMISSION RESEARCH AT MSFC	
by James T. Powell	1
NARROW BAND OPTICAL FILTERS FOR SOLAR OBSERVATIONS	
by Preston L. Hassler, Jr.	
SUMMARY	3
INTRODUCTION	3
SOLAR OBSERVATION	3
FILTER CHARACTERISTICS	4
INTERFERENCE FILTERS	4
BIREFRINGENT FILTERS	7
FILTERS FOR ATM	7
REFERENCE	8

LIST OF TABLES

Table	Title	Page
I.	Comparison of Birefringent and Interference Filters	7
II.	Improvements in Interference Filters	8

LIST OF ILLUSTRATIONS

Figure	Title	Page
1.	Solar Spectrum	3
2.	Hydrogen-Alpha Region of the Solar Spectrum	4
3.	Photograph of the Sun at the Hydrogen-Alpha Frequency	4
4.	Typical Filter Response	5
5.	Interference Filter Optical Diagram	5

CONTENTS (Continued) . . .

Figure	Title	Page
6.	Wave Amplitude Derivation	6
7.	Vector Diagrams of Transmitted Waves	6
8.	Filter Transmission Curves	6
9.	Effect of Reflectance	6
10.	Filter Response to Tilt	7

AN ORBITING SYSTEM FOR THE IDENTIFICATION AND MEASUREMENT OF GALACTIC X-RAY SOURCES

by Stephen D. Rose

SUMMARY	9
INTRODUCTION	9
X-RAY DETECTOR	10
RADIATION DETECTION PROCEDURE	15
CONCLUSION	17
REFERENCES	17

LIST OF ILLUSTRATIONS

Figure	Title	Page
1.	An Identified X-ray Source, Crab Nebula	9
2.	S-027 X-ray Astronomy Experiment Package	10
3.	Supporting Electronics for S-027 Experiment	11
4.	Sensor Package Top Surface	11
5.	Collimator	11
6.	Collimator Field of View	11
7.	Proportional Counter Array in the Sensor Package	12
8.	X-ray Photon Ionization in the Proportional Counter	12
9.	S-027 Experiment Block Diagram	13

CONTENTS (Continued) . . .

Figure	Title	Page
10.	Proportional Counter Pulse to be Analyzed	13
11.	Scintillator Box	14
12.	X-ray Pulse Analysis	14
13.	Star Tracker Assembly	15
14.	Star Sensor Field of View Related to the Collimator Field of View	15
15.	Sensor Package on a Controlled Temperature Plate in a Saturn IU	16
16.	S-027 Experiment View Angle.	16
17.	S-027 Experiment Orientation on the Scanning Orbits	16

DEVELOPMENT OF AM BASEBAND TELEMETRY TECHNIQUES FOR WIDEBAND DATA

by Frank H. Emens

INTRODUCTION.	19
AM BASEBAND TELEMETRY SYSTEMS	19
Generation of DSB	23
Automatic Gain Control.	23
Carrier Synthesis.	24
Demodulation of DSB.	24
Square Wave Modulators	24
Tape Speed Fluctuations	25
CONCLUSIONS.	26
FUTURE PLANS	26

LIST OF TABLES

Table	Title	Page
I.	Comparison of RF Bandwidth Utilization Efficiency.	19
II.	Nominal Channel Bandwidths.	23

LIST OF ILLUSTRATIONS

Figure	Title	Page
1.	Channel Response versus Signal/Noise Ratio for a Given Channel Location.	20
2.	Electromechanical Bandpass Filter for Saturn SS-FM Telemetry System	21

CONTENTS (Continued) . . .

Figure	Title	Page
3.	Saturn SS-FM Telemetry System	22
4.	Idealized DSB Multiplexer	23
5.	Idealized DSB Demultiplexer	24

REDUNDANCY REMOVAL TECHNIQUES FOR COMPRESSION OF TELEMETRY DATA

by Gabriel R. Wallace

SUMMARY	27
INTRODUCTION	27
INFLIGHT REDUNDANCY REMOVAL	28
Algorithm Notation	28
Algorithm Operations	28
JUPITER DATA REDUNDANCY STUDY	36
BREADBOARD DEVELOPMENT OF SIMPLE (ZFN) ALGORITHM DEVICE	36
ZFN FLIGHT UNIT DEVELOPMENT AND FABRICATION	37
COMPUTER STUDIES OF REAL AND SIMULATED DATA	39
RECENT DEVELOPMENT IN HARDWARE	44
CONCLUSIONS	45
REFERENCES	45
BIBLIOGRAPHY	46

LIST OF ILLUSTRATIONS

Figure	Title	Page
1.	Representative Data Spectra ($1/2 f_c$ rate)	27
2.	Representative Data Spectra (Actual Rate)	27
3.	Representative Data Spectra (Actual Rate)	27
4.	Zero Order, Fixed Corridor, Nonredundant Sample Transmitted (ZFN)	29
5.	Zero Order, Variable Corridor, Preceding Sample Transmitted (ZVP)	30

CONTENTS (Concluded) . . .

Figure	Title	Page
6.	Zero Order, Variable Corridor, Artificial Preceding Sample Transmitted (ZVA)	31
7.	First Order, Fixed Corridor, Nonredundant Sample Transmitted (FFN)	32
8.	First Order, Fixed Corridor, Preceding Sample Transmitted (FFP)	33
9.	First Order, Fixed Corridor, Artificial Preceding Sample Transmitted (FFA)	34
10.	First Order, Variable Corridor, Preceding Sample Transmitted (FVP)	35
11.	First Order, Variable Corridor, Artificial Preceding Sample Transmitted (FVA)	36
12.	ZFN Airborne Redundancy Removal Unit	37
13.	Functional Block Diagram of the Telemetry Data Compressor	38
14.	Error (rms) Versus Compression Ratio for the 5th Order Data (RSR=10)	39
15.	Error (rms) Versus Compression Ratio for SA-7 Temperature Measurements	40
16.	Error (rms) Versus Compression Ratio for SA-8 Temperature Measurements	40
17.	Error (rms) Versus Compression Ratio for SA-9 Temperature Measurements	41
18.	Error (rms) Versus Compression Ratio for SA-10 Temperature Measurements	41
19.	Error (rms) Versus Compression Ratio for SA-7 Pressure Measurements	42
20.	Error (rms) Versus Compression Ratio for SA-8 Pressure Measurements	42
21.	Error (rms) Versus Compression Ratio for SA-9 Pressure Measurements	43
22.	Error (rms) Versus Compression Ratio for SA-10 Pressure Measurements	43
23.	Telemetry Redundancy Analyzer	44

INTRODUCTION TO AIRBORNE INSTRUMENTATION AND DATA TRANSMISSION RESEARCH AT MSFC

By

James T. Powell

The Instrumentation and Communication Division of the Astrionics Laboratory has the responsibility for data management systems for the collection, encoding, and transmission of data. As space flight missions become more sophisticated, the data management systems to support these missions become correspondingly more complex. It thus becomes increasingly more difficult, but more necessary, to maintain a "systems approach." This is also true of supporting research and technology projects. The Astrionics Laboratory conducts research, design, and development related to tracking, command, instrumentation, and telemetry systems in support of assigned and anticipated MSFC projects. Every effort is made to conduct a broad range of research and

development activity composed of interrelated tasks. The choice of these tasks is based on the experience gained with current systems hardware and must be made in the context of overall mission and system requirements as projected for future missions. Individual tasks are directed to solving specific aspects of the overall data management systems, and together these tasks fit into a mosaic that represents a well-considered systems approach. The Astrionics Laboratory's data systems, beginning with the Redstone missile, have provided consistently reliable, accurate data and have contributed several significant advances to current technology. This review describes only a few of the more interesting projects.

NARROW BAND FABRY-PEROT FILTERS FOR SOLAR OBSERVATIONS

By

Preston L. Hassler, Jr.

SUMMARY

The operation and characteristics of narrow band optical filters are discussed. New filter fabrication techniques and solar observations with narrow band filters are mentioned. These filters are designed to study a 0.5 and 1.0 Å wavelength range at the H- α line in the solar spectrum.

INTRODUCTION

The Apollo Telescope Mount (ATM) will have five astronaut-operated experiments to gather scientific data from the sun. In addition the ATM will provide two telescopes for solar patrol. These two telescopes will be used by the astronaut to locate and monitor solar disturbances. A narrow band optical filter is necessary to permit distinction of these disturbances in the visible wavelengths. This paper discusses these narrow band optical filters.

SOLAR OBSERVATION

Radiant energy received from the sun contains many wavelengths in the visible spectrum. Narrow band optical filters limit the range of these wavelengths that can enter a telescope. By using optical filters to select only certain wavelengths, the astronaut can study those wavelengths that offer the best information.

Figure 1 is a curve of the solar spectrum. The horizontal axis shows the wavelength or frequency of the radiation. The vertical axis indicates the energy radiated by the sun at various wavelengths. This solar spectrum covers about 18 000 Å (the visible spectrum is about 3000 Å wide).

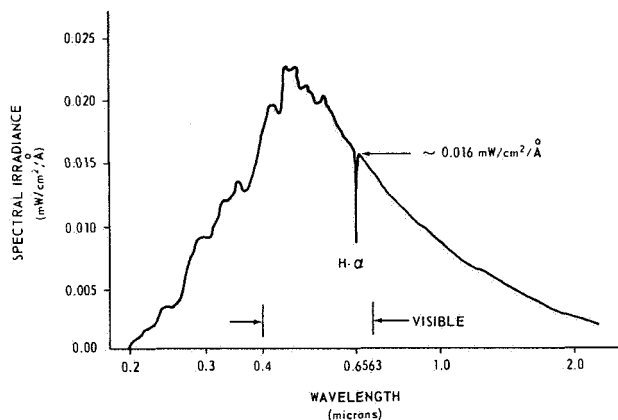


FIGURE 1. SOLAR SPECTRUM

There are several dips and peaks in the solar spectrum. In one of the dips, the hydrogen-alpha (H- α) line, solar observations are very revealing. The H- α line occurs at a wavelength of 6563 Å in the visible red region of the spectrum. Figure 2 is a small part of the sun's spectrum that spans only 7 Å and is centered on the dip at the H- α line. Also centered on the dip at the H- α line are three other curves of higher energy levels; these curves represent the energy outputs of certain types of solar occurrences. Different types of solar occurrences are distinguished by the different amounts of energy detectable with the narrow band filters at the H- α line. The greatest amounts of energy detected at the H- α line have been associated with large flares; smaller amounts with small flares; and amounts that are only slightly above the normal solar level have been associated with plage areas. Other solar occurrences, sunspots, and filaments can be detected by their complete lack of energy in the H- α region. Bandwidths of 0.5, 1.0, and 2.0 Å are also shown in Figure 2.

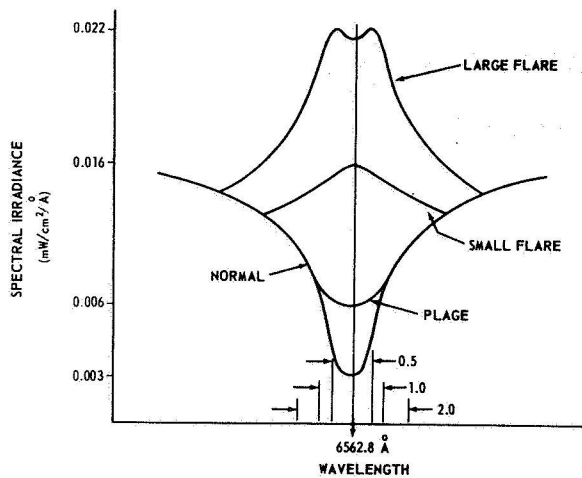


FIGURE 2. HYDROGEN-ALPHA REGION OF THE SOLAR SPECTRUM

A photograph made by the High Altitude Observatory is shown in Figure 3. It was made with a narrow bandpass filter centered at the H- α line. The bandwidth of the filter was 0.5 Å. Solar

occurrences visible in the photograph are filaments, sunspots, plage areas and flares. The mottled area is the undisturbed sun.

FILTER CHARACTERISTICS

Filters used in acquiring pictures such as Figure 3 have similar transmission curves as shown in Figure 4. The peak transmission of narrow band filters varies from 5% to 40% depending upon the type of filter and the materials used. The wavelength where peak transmission occurs is called the center wavelength, λ_0 . The filter bandwidth, which is measured across the $\frac{1}{2}$ power points, is typically 0.4 to 1.0 Å. The shaded areas in Figure 4 are called the wings of the filter. The wings are minimized as much as possible.

INTERFERENCE FILTERS

Two types of narrow band filters are the interference or Fabry-Perot filter and the birefringent

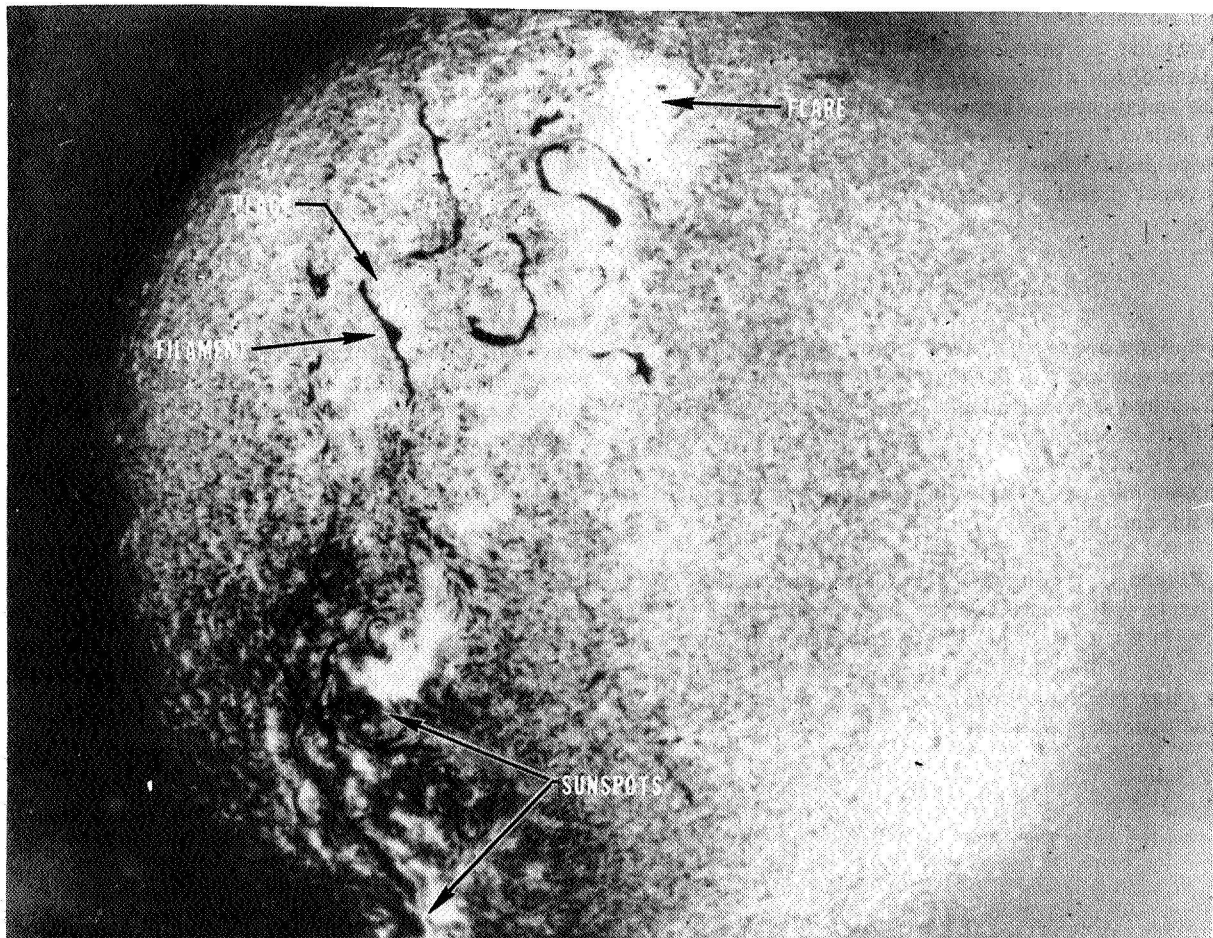


FIGURE 3. PHOTOGRAPH OF THE SUN AT THE HYDROGEN-ALPHA FREQUENCY

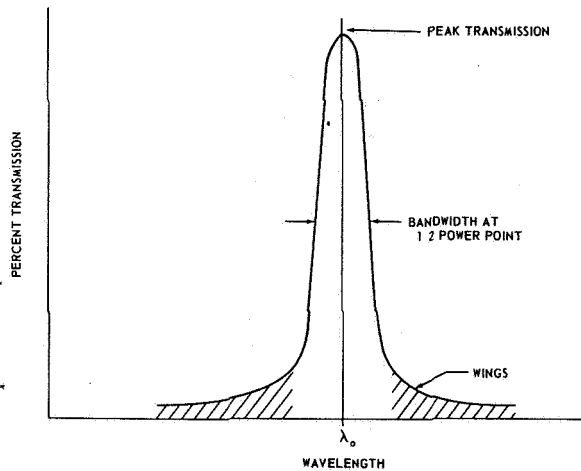


FIGURE 4. TYPICAL FILTER RESPONSE

or Lyot filter. Construction of the interference filter can be accomplished in several ways. Basically the filter has two highly reflective surfaces separated by a space or spacer. In some filters the reflective coatings are placed on both sides of a thin film or thin material (sheet of mica) that serves as the spacer. Another technique is to coat a flat piece of glass and optically contact another piece of glass to this coated surface. This second piece of glass is polished very thin, is coated, and serves as the spacer between the two reflective coatings.

The spacer between the reflective coatings has a thickness that corresponds to a phase shift of π (or an integral number times π) for the center wavelength λ_0 [1]. This means that the transmitted light, λ_0 , has a phase advance of π while passing straight through the filter. In Figure 5, the lines are purposely drawn at an angle for clarity. When light beam *a* strikes the first surface, some of the light beam *a* reflects, *b*, and the balance is transmitted, *c*. Light beam *b* undergoes a phase shift of π during reflection because it is passing from a low density medium to a higher density medium. Light beam *c* is transmitted through the filter and arrives at the second surface with a phase advance of π . Some of light beam *c* reflects, *e*, and part goes through, *d*. Light beam *d* is the first of many beams to be transmitted through the second surface.

Light beam *e*, which was reflected from the second surface, returns to the first surface. Some of the light beam *e* is transmitted, *f*, and part reflects, *g*. Light beam *f* has gone through a total phase advance of 2π from the original incoming wave.

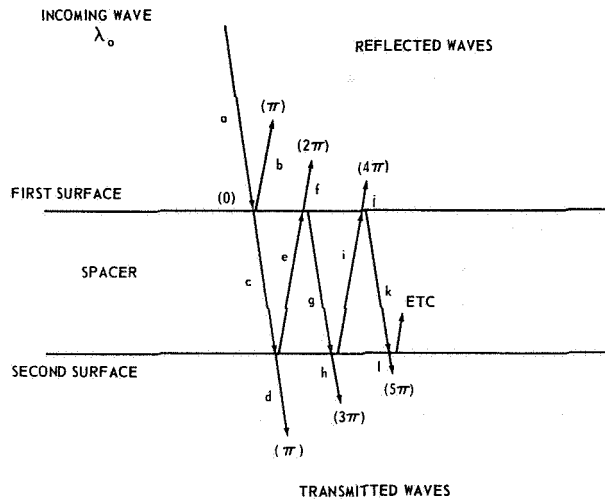


FIGURE 5. INTERFERENCE FILTER OPTICAL DIAGRAM

The first reflected wave, *b*, has a phase shift of 1π . So the two waves that return toward the source have a phase difference of $2\pi - 1\pi$, or π . They are out of phase with each other and therefore have cancelling effects. Reflected light beam *g* returns to the second surface. Part of *g* is transmitted, *h*, and part of *g* is reflected, *i*. Light beam *h* has undergone a phase advance of 3π from the original wave, and an advance of $3\pi - 1\pi$, or 2π from the first transmitted wave. The two transmitted waves are in phase and reinforce (add amplitudes). It is evident that all transmitted waves of λ_0 light are in phase with each other, and all reflected waves except the first are in phase with each other. The amplitudes of these waves can be calculated by multiplying the amplitude of the original wave by the coefficients of reflection and transmission each time the wave was reflected or transmitted. A general equation can be derived for the reflected and transmitted waves (Fig. 6). In both cases each succeeding wave has an amplitude decrease equal to the product of the internal reflection coefficients. If on the first surface the transmission and reflection coefficients are coated for the optimum, then all the reflected waves will cancel out. Theoretically, by the law of conservation of energy, all the light of λ_0 would be transmitted. In the practical case this is not possible because of absorption and scattering losses in the spacer and coating mediums.

An incoming wave with a wavelength different from λ_0 would have a phase advance different from π . These phase advances will be $\pi \pm \Delta$, depending on

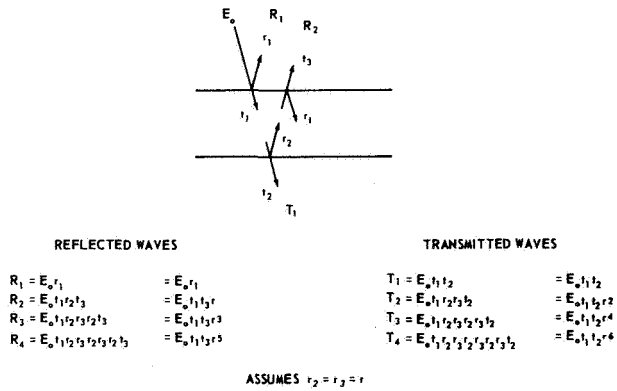


FIGURE 6. WAVE AMPLITUDE DERIVATION

whether the new λ is shorter or longer than λ_0 , respectively. To visualize the phase advances, a vector summation diagram can be drawn. For the transmitted waves, the phase of the first wave was π , and the phases of succeeding waves were 2π greater. When a greater phase advance occurs, then Δ would be added to π so that the first wave is $\pi + \Delta$, the second $3(\pi + \Delta)$, the third $5(\pi + \Delta)$, etc. The phase difference between waves is always $2n\pi + 2\Delta$, where n is always a whole number that depends upon the thickness of the spacer. Figure 7 shows a vector summation diagram for $\Delta = 0$, $\Delta = 22.5^\circ$, and $\Delta = 45^\circ$. When $\Delta > 0$ the vector is plotted at an angle of 2Δ from the preceding wave since 2Δ is the phase difference between any two adjoining waves. As Δ gets larger, the sum of the vectors gets smaller. This is the case up to $\Delta = 90^\circ$ where $2\Delta = 180^\circ$, or worst out-of-phase condition. After that the waves will start becoming more in phase with each other. Therefore an interference filter actually has a transmission curve as shown in Figure 8.

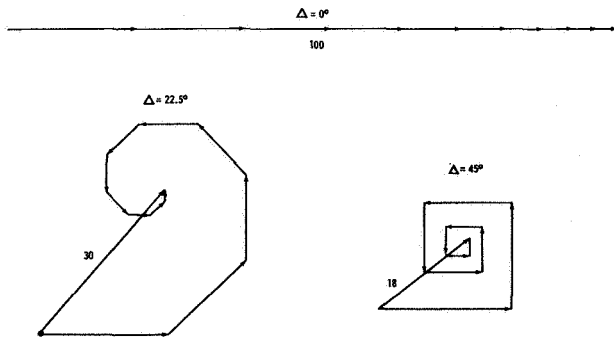


FIGURE 7. VECTOR DIAGRAMS OF TRANSMITTED WAVES

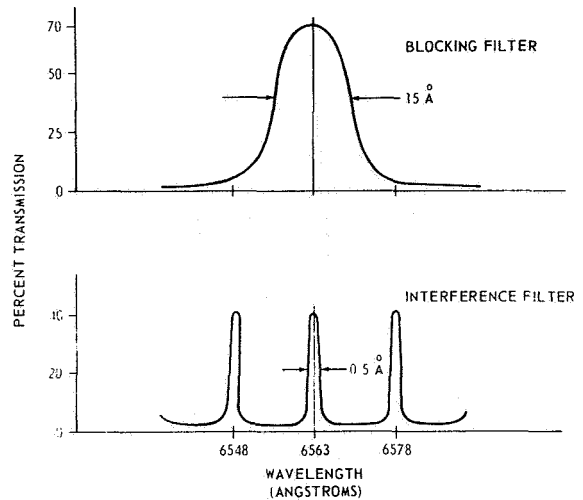


FIGURE 8. FILTER TRANSMISSION CURVES

The thinner the film or spacer between the two reflective surfaces, the further apart adjacent wave peaks will be. Typical filters now have adjacent wave peaks approximately 15 \AA apart in the H- α region. As the wavelength under consideration gets longer (or red), the peaks would be further apart. Shorter wavelengths (more blue) have peaks closer together. Since light from only one of these peaks must enter the telescope, a blocking filter is needed. This blocking filter has a bandwidth just wide enough to exclude the adjacent wave peaks on each side of the center wavelength.

If the fact of reflectance of the two surfaces is considered, the curve shown in Figure 9 is typical. Thus as the surfaces are made more reflective, more of the off-center light is rejected, but the center wavelength essentially is not affected.

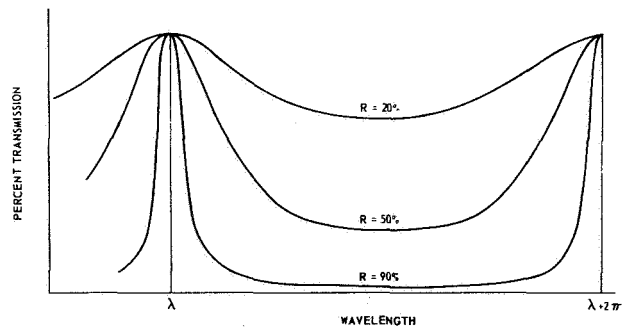


FIGURE 9. EFFECT OF REFLECTANCE

Since the critical factor in these filters is the optical pathlength in the spacer, then the center frequency can be varied by changing this pathlength. This is done either one of two ways: thermally or by tilting the filter. Temperature changes cause the material to contract or expand, thus causing the optical pathlength to change. If the filter is tilted, the pathlength can be increased but not decreased from the straight-through pathlength. Typical frequency variation with tilt is shown in Figure 10. Variation in the center frequency may or may not be desired, depending upon the application. The temperature coefficient is 0.05 Å shift/°C. Thermal conditioning would be a definite consideration to prevent drift or to tune the filter. The temperature would have to be changed ±10°C to move the filter ±0.5 Å.

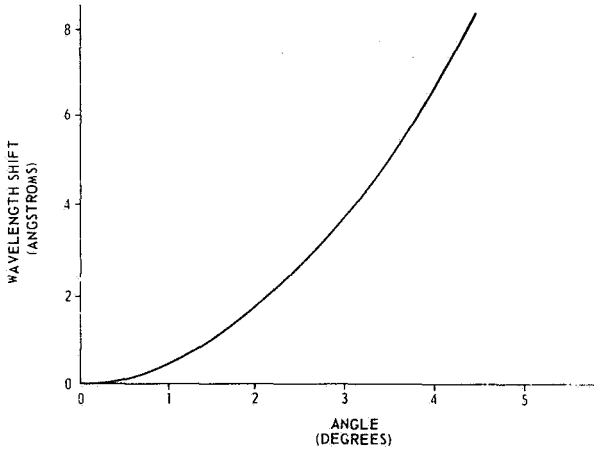


FIGURE 10. FILTER RESPONSE TO TILT

BIREFRINGENT FILTERS

The second type of filter, the birefringent filter, consists of approximately eight calcite plates. There is a polaroid filter between each of the plates. Each plate is twice as thick as the preceding plate. For a narrower filter bandwidth, thicker plates must be added. Two factors cause the practical limit on the bandwidth to be approximately 0.5 Å: efficiency of the filter (as low as 5%), and the size of material available. The availability of good calcite crystals limits the production of these filters and causes them to be rather expensive. The birefringent filter is

very temperature sensitive. It has a spectral change of ~ 0.4 Å/°C. Therefore, for a constant filter center wavelength, the temperature would have to be controlled to better than 0.1 °C for a 0.5 Å observation.

For space use, the interference filter has several advantages over the birefringent filter (Table I). It is more efficient, less temperature sensitive, and lighter in mass.

TABLE I. COMPARISON OF BIREFRINGENT AND INTERFERENCE FILTERS

	Birefringent	Interference
Bandwidth	0.5 Å	0.5 Å
Efficiency	5%	40%
Thermal Sensitivity	0.37 Å/°C	0.05 Å/°C
Aperture Diameter	2.54 cm (1.0 in.)	5.1 - 7.6 cm (2-3 in.)
Weight	1.36 kg (3 lb)	0.45 kg (1 lb)
Cost (Approx)	\$15, 000	\$3, 000

FILTERS FOR ATM

The ATM program includes two telescopes that are specifically designed for use at the H-α line. One telescope has a 0.5 Å bandpass filter and the other has a 1.0 Å bandpass filter. Both telescopes are used for locating solar phenomena. The telescope with the 0.5 Å filter gives the greatest detail of solar structure for general observations. The telescope with the 1.0 Å filter is used to discover flares more easily and quickly. With a wider filter bandpass most of the details on the sun do not radiate enough energy to be discriminated from the normal solar background. However, flares, which are the most powerful radiators at H-α, can still be discriminated from the solar background. If the filter bandwidth was allowed to get wider, beyond 2 Å, the flares would be very hard to find except when they were extremely large.

At the beginning of the ATM program, the only suitable filters were the birefringent types. However, they were not very desirable because of their low efficiency, high temperature sensitivity, and long lead time. Some work had been done with interference type filters, but they were still considered undesirable because the bandpasses were too wide. When using interference filters, the

center wavelength would shift with time because adhesives that were used in the filters were affected by temperature changes. Since then a new technique for adhesion in filters has been used. The glass pieces are polished so flat that they adhere to each other by molecular adhesion. This is accomplished by polishing the glass, checking its flatness with interference techniques, and repolishing until the desired flatness is obtained.

Because of the new techniques that allow the use of glass, the interference filters have several improved characteristics (Table II). Previously the best filters were made by depositing reflective coatings on mica substrates. The thickness of mica is very consistent over an area comparable to filter sizes. However, mica absorbs more light than glass and is therefore a less efficient material. Also, larger pieces of mica of good optical quality are difficult to obtain. Thus the aperture diameter was limited to approximately 2.54 cm (1.0 in.). Coating and measuring techniques are improving, and this permits narrower bandwidths. The possibilities of filters with bandpasses smaller than 0.1 Å seem very good. These type filters can be used to study the magnetic effects on the solar gases.

The telescopes and fused-silica narrow-band filters for use at the H- α line are being designed and fabricated by the Perkin Elmer Corp., Wilton, Connecticut, for NASA under contract NAS 8-22623.

TABLE II. IMPROVEMENTS IN INTERFERENCE FILTERS

	1967	1968
Material	Mica	Glass
Bandwidth	0.7 - 0.9 Å	0.1 - 0.5 Å
Efficiency	20%	40%
Aperture Diameter	2.54 cm (1.0 in.)	5.1 - 7.6 cm (2-3 in.)

REFERENCE

1. Born, Max; and Wolf, Emil: Principles of Optics. The McMillan Company, 2nd Revised Edition, 1964, paragraph 7.6.1, pp. 323-329.

AN ORBITING SYSTEM FOR THE IDENTIFICATION AND MEASUREMENT OF GALACTIC X-RAY SOURCES

By

Stephen D. Rose

SUMMARY

This discussion will outline the development and construction of an orbiting X-ray sensor. This X-ray sensor is to be flown in a Saturn Instrument Unit and will scan a portion of the sky for X-ray sources of low flux.

The detector system is being built for MSFC by the University of Wisconsin. The Principal Investigators are Drs. William L. Kraushaar and Frank Scherb of the Department of Physics at the University of Wisconsin. Design and fabrication of the sensor package are being done under subcontract to the University of Wisconsin by Space Craft, Inc., in Huntsville, Alabama.

Observation of X-ray sources outside of the solar system can be accomplished only by detectors placed above the atmosphere of the earth. So far, X-ray measurements taken over small portions of the sky have been made strictly by balloon or sounding-rocket-borne measuring systems. Because balloons have an altitude limit, most measurements of the sky have been made from rockets. But rocket measurements are also limited by the payload size they can carry and by short observing times. The result is that only a small area of the sky can be examined on each flight so that only a meager amount of data is now available. X-ray astronomy needs an orbital observing system that could scan a larger portion of the sky with high sensitivity and map the location of any detected X-ray sources.

INTRODUCTION

X-ray astronomy, an important area of scientific investigation, is still in its infancy and bears a resemblance to the early state of radio astronomy. The major obstacle in the development of X-ray astronomy is that the earth's atmosphere is opaque to soft X-rays. This situation prohibits land based

observation of galactic X-ray emitters. However, with the beginning of the U.S. space program, space scientists began placing X-ray detecting instrumentation on sounding rockets to get above the earth's atmosphere to search the sky for sources of X-rays.

In 1962, a team of MIT scientists assisted by the American Science and Engineering (ASE) Corp. detected X-rays from outside the solar system by a rocket launched from the White Sands Missile Range, White Sands, New Mexico [1]. This flight provided the first evidence of a detectable flux of soft radiation from beyond the solar system. The evidence from this flight stimulated the development of X-ray astronomy and rapid progress has been made by three different groups of experimenters. In addition to the ASE-MIT group, these experimenters include the Naval Research Laboratory and Lockheed Aircraft. More than a dozen discrete X-ray sources have now been observed.

Aside from the sun, only two known stellar objects have been identified as being sources of X-rays. Perhaps the best known emitter is the Crab Nebula shown in Figure 1. The strongest

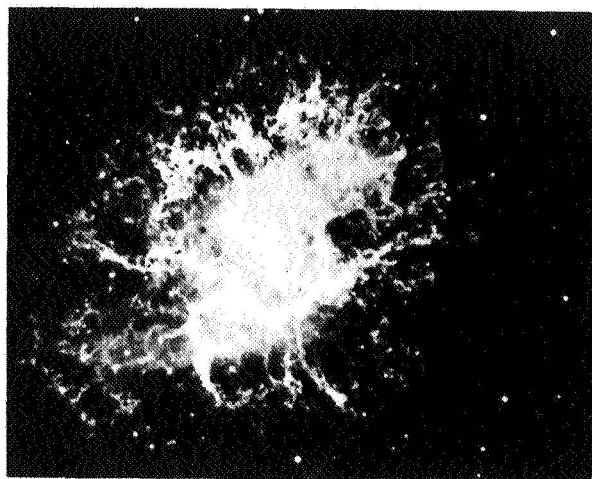


FIGURE 1. AN IDENTIFIED X-RAY SOURCE, CRAB NEBULA

source to have been discovered is a faint star in the constellation Scorpius designated Sco XR-1. The remaining sources are still unidentified as far as being associated with optical or radio objects. Further optical identifications await high resolution X-ray detection instruments and/or lunar occultation measurements.

All of the experimental information accumulated from previous rocket flights does not tell much about the emission mechanisms of the identified sources, or their exact location, or their exact angular diameter. The existence of a general X-ray background is suspected but not verified. It is known that the Sagittarius region is a bright source of X-rays, but whether this brightness results from many unresolved discrete sources or from general nebulosity is not known. Rocket flights have observed a spectral range of radiation from 0.5 - 15 Å and known X-ray sources have flux values greater than 0.1 photons $\text{cm}^{-2} \text{s}^{-1}$, which is the present lower limit of detection, and most of them seem to be concentrated near the galactic plane [2]. It is probable that weaker sources exist. More experimental work is needed to understand the nature of the observed sources and to do a survey of the sky with greater completeness and higher sensitivity. It will be particularly interesting to measure the spectrum of each source since it is intimately related to the X-ray production mechanism. Also, since interstellar absorption becomes appreciable at longer wavelengths, spectrum measurements that extend to the 10 to 50 Å region can help in determining the distance of sources. Accurate determination of the celestial location of the sources will permit a careful search for visible and radio emissions.

The immediate objective is to obtain a high sensitivity mapping of a portion of the sky to determine the spatial distribution of any detected sources. A secondary objective is an attempt to establish whether a general background radiation actually exists. In addition, limited spectral information will be obtained with proportional counters [3].

X-RAY DETECTOR

The X-ray detector (Fig. 2) is similar to one that would be flown on a sounding-rocket except that its sensing surface is much larger. The sensor package consists of a collimator to restrict the field of view, an array of ten gas-filled proportional counters, a plastic scintillator enclosing the proportional counter array to detect and veto possible false

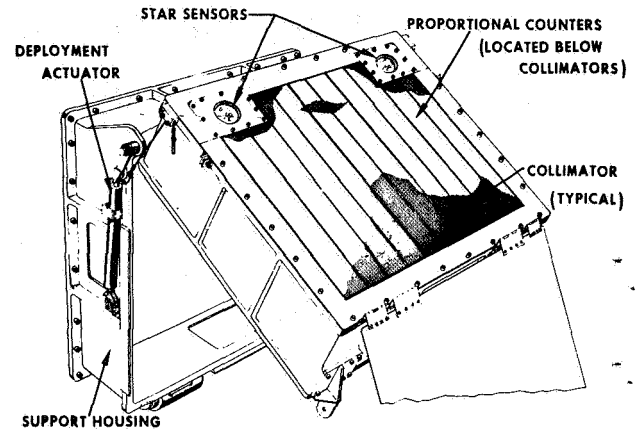


FIGURE 2. S-027 X-RAY ASTRONOMY EXPERIMENT PACKAGE

counter outputs caused by high energy cosmic rays, two star trackers that assist in identification of possible X-ray sources when their output is correlated with the counter data, and the supporting electronics [4]. In addition, an auxiliary storage and playback unit is incorporated into the Instrument Unit telemetry system to store experiment output data on a tape recorder for later playback to a ground station.

The supporting electronics are mounted on a baseplate that divides the sensor into two parts. The bottom section shown in Figure 3 contains signal amplifiers, power supplies, both digital and analog signal conditioning equipment, and an output buffer. The top section contains the scintillator and X-ray detector. All of this equipment, including the radiation sensors and electronics, is contained in a self-supporting casting 63.4 cm (25 in.) on each side and 30.5 cm (12 in.) deep, which is attached to the Saturn Instrument Unit by a deployment mechanism.

The collimator is mounted on the sensor casting as shown in Figure 4. It is contained in a flange-mounted self-supporting box frame 5.08 cm (2 in.) deep. The sensing area is a 50.8 cm (20 in.) square opening in the box frame. This opening is partitioned with structural members into ten smaller collimators 5.08 cm (2 in.) wide that are centered over a proportional counter of approximately the same size. Four of these smaller compartments are shortened by 8.9 cm (3.5 in.) to provide space for the star trackers.

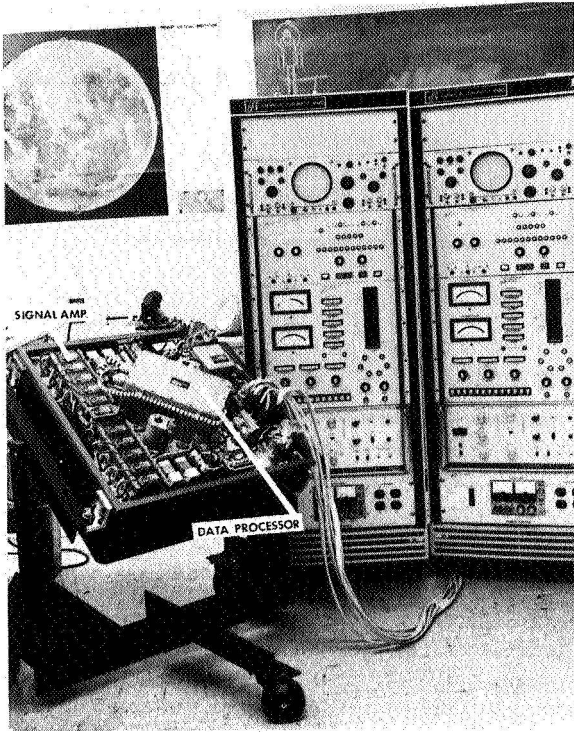
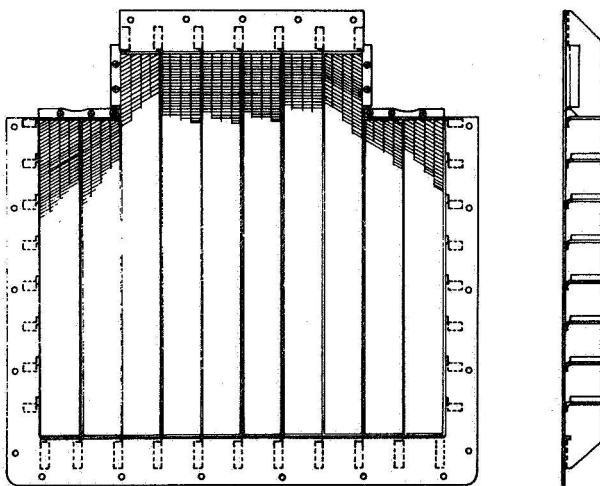


FIGURE 3. SUPPORT ELECTRONICS

Each of these ten major structural compartments is further subdivided over the entire length with thin copper fins spaced 0.0157 cm (0.062 in.) apart. Figure 5 shows a top view of these copper fins. As



COLLIMATOR BOX TOP VIEW

FIGURE 5. COLLIMATOR

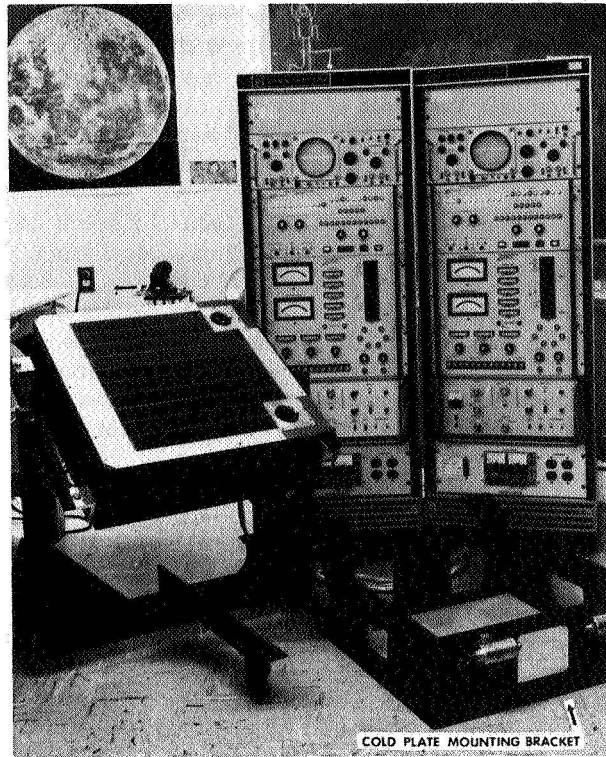


FIGURE 4. SENSOR PACKAGE TOP SURFACE

can be seen, six of the ten sub-compartments have the fins placed at a 45 degree angle to the main dividers while the other four have the fins at a 90 degree angle. The fins result in a basic structure which is either a 45 degree or a 90 degree parallelepiped 5.17 cm (2 in.) deep.

The total collimator field of view essentially consists of three slits that project onto the celestial sphere (Fig. 6). Two of the slits formed by the

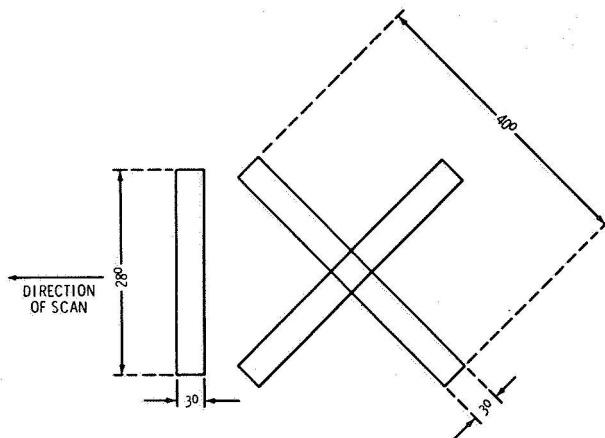


FIGURE 6. COLLIMATOR FIELD OF VIEW

45 degree fins have orthogonal projections of 40 degrees by 3 degrees. The third slit formed by the 90 degree fins has a projection of 28 degrees by 3 degrees. This field of view was chosen because it represents an optimum tradeoff between sensitivity and accuracy in locating X-ray sources.

X-ray detection is accomplished by means of an array of ten 0.00508 cm (0.002 in.) beryllium-window argon-filled proportional counters. A beryllium window is highly transparent to X-rays in the 1.7 - 12 Å wavelength region of interest. As shown in Figure 7, the window is supported by a screen-like structural member that provides the window with enough strength to withstand the vacuum of space.

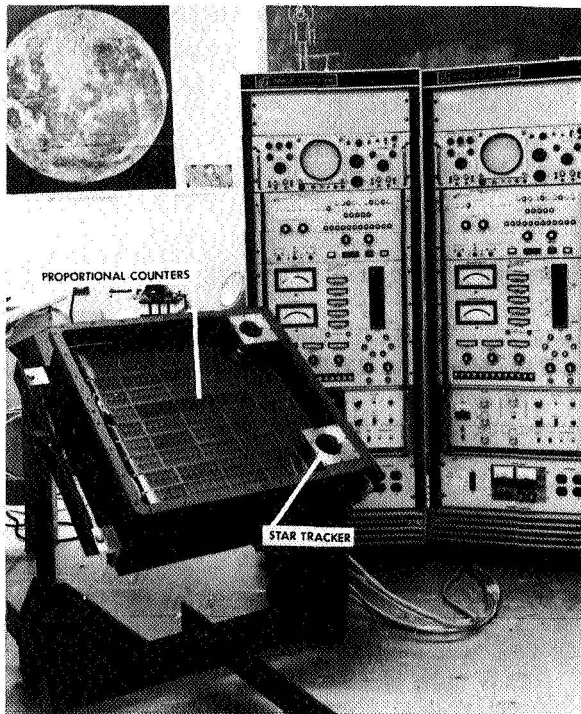


FIGURE 7. PROPORTIONAL COUNTER ARRAY IN THE SENSOR PACKAGE

As shown in Figure 8, an X-ray photon entering the proportional counter chamber ionizes the argon gas, forming a number of ion pairs directly proportional to the photon energy. The primary ion pairs, i.e., electrons and positively charged gas molecules, are accelerated by an intense electric field between a fine wire center electrode and the chamber wall.

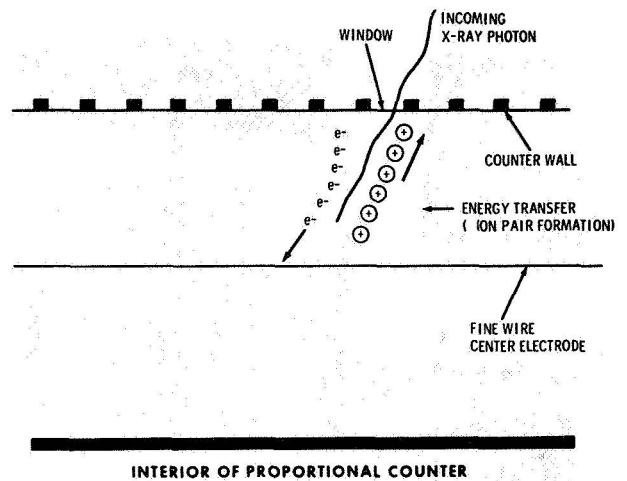


FIGURE 8. X-RAY PHOTON IONIZATION IN THE PROPORTIONAL COUNTER

As the electrons move toward the positively charged center electrode, they collide with and ionize other gas molecules. The additional electrons produced by these collisions amplify the original energy transfer. The positively charged center electrode then collects the electrons and converts them to a pulse of electrical current that is proportional to the energy of the photon, and a larger more usable signal can be emitted by the counter.

Charge sensitive amplifiers process each detector output into a differential pulse height analyzer in which a single input pulse is analyzed. A count is registered in only one binary scalar covering the band of pulse heights or energy into which the pulse falls. The analyzing is accomplished by a parallel-input five-level discriminator. The block diagram of Figure 9 shows the signal conditioning equipment needed to process each input signal.

As the incoming pulse rises to its maximum, it triggers the discriminators in ascending order. Each discriminator must temporarily retain its triggered level until the pulse has had time to reach a peak. Then a strobe pulse is generated to scan the output gates and dump a count into the appropriate register.

Note that the pulse shown in Figure 10 falls in energy band 4. This is true because the electronics record a count when the pulse has reached 90% of its maximum height. Therefore, a count is recorded in binary scalar number.

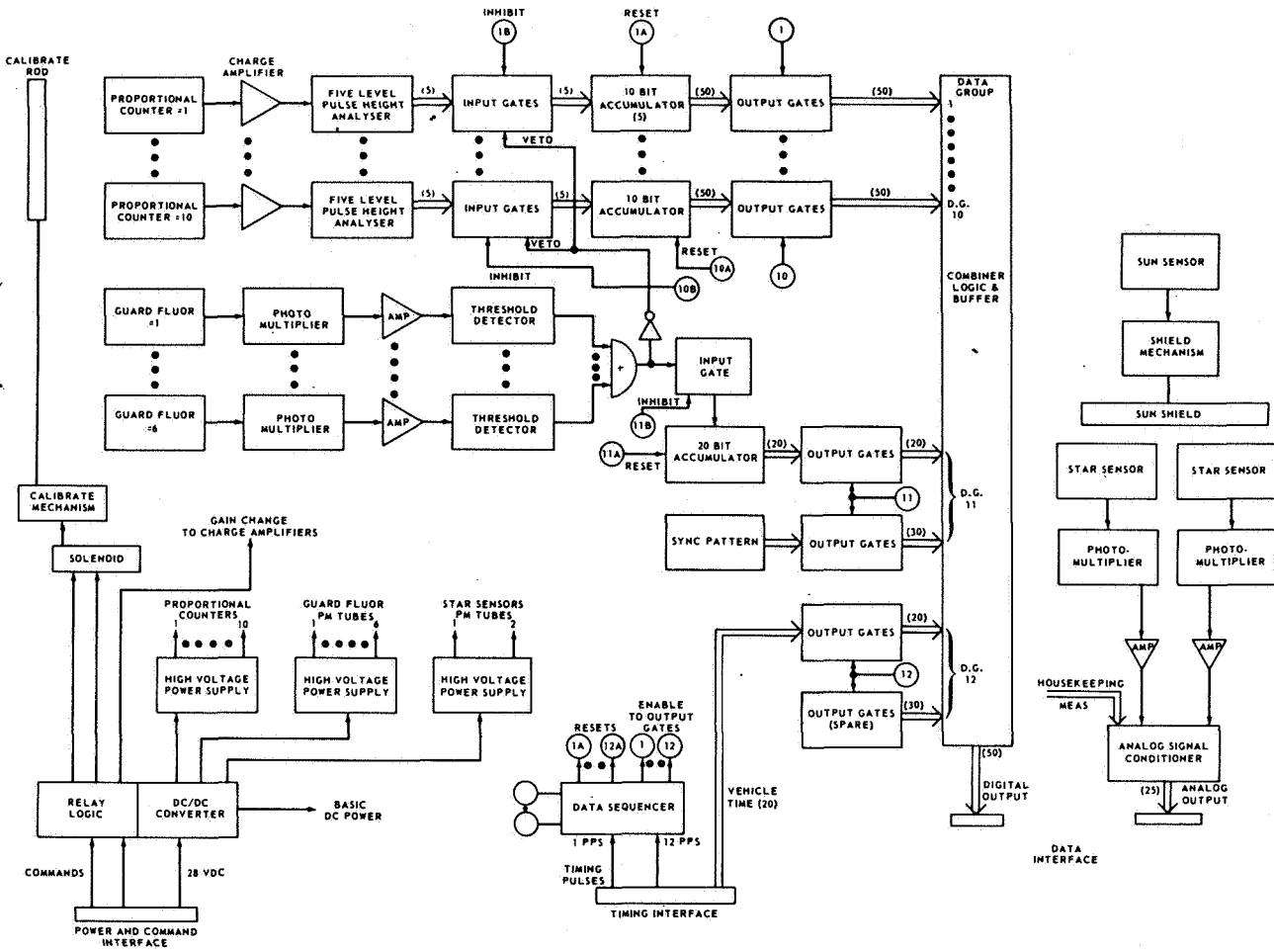


FIGURE 9. S-027 EXPERIMENT BLOCK DIAGRAM

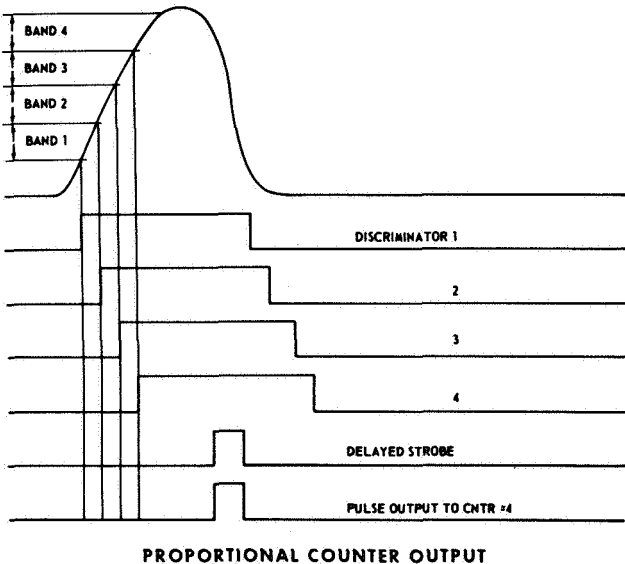


FIGURE 10. PROPORTIONAL COUNTER PULSE TO BE ANALYZED

Gating is accomplished by having each successively higher discriminator inhibit the counter gate for the next lowest discriminator output; thus, the only gate remaining open is the one associated with the highest level discriminator.

A plastic scintillator (Fig. 11) in the form of a five-sided box surrounds the proportional counter array on the five nonsensing surfaces to provide an anti-coincidence signal. Energetic cosmic rays that deposit energy in the active volume of the proportional counters will also penetrate the scintillator.

The resulting ionization of the scintillator produces a pulse of light. X-rays with wavelengths of from 1.7 - 12 Å will not penetrate both the proportional counter and the fluorguard box. All surfaces of the scintillator box are polished and a coat of diffusive white paint covers all inactive surfaces to scatter light. Photomultiplier tubes view the four sides and bottom of the box. The anti-coincidence

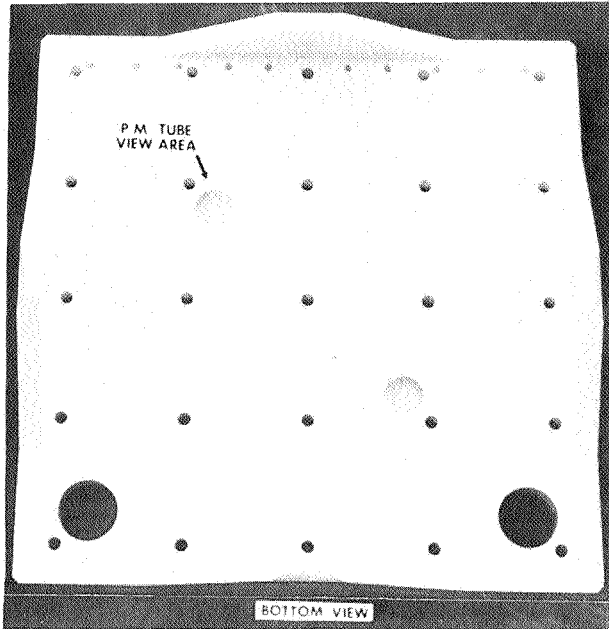


FIGURE 11. SCINTILLATOR BOX

scintillations are picked up by the photomultipliers whose outputs are amplified and used in the data handling system to prevent false counter indications.

A ten-bit binary accumulator follows each pulse height analyzer level for temporary storage of the counter outputs. The accumulators are grouped to count pulses from each of the five levels of the pulse height analyzer associated with one proportional counter. An input gate is provided to inhibit the counter during readout and to veto counts from the analyzer when in coincidence with pulses from the fluorguard surrounding the proportional counter. The drawings in Figure 12 illustrate the analysis of an incoming pulse. The top diagram in the figure represents a counter output displayed on a 128 channel analyzer. The source here is a Fe^{55} X-ray source that emits a radiation having a wavelength of 2 \AA and an energy of 5 KeV. The middle diagram shows the same counter output displayed from the five channel analyzer including counts from a cosmic ray background. The bottom diagram shows the stored counts in the accumulators of the five channel analyzer

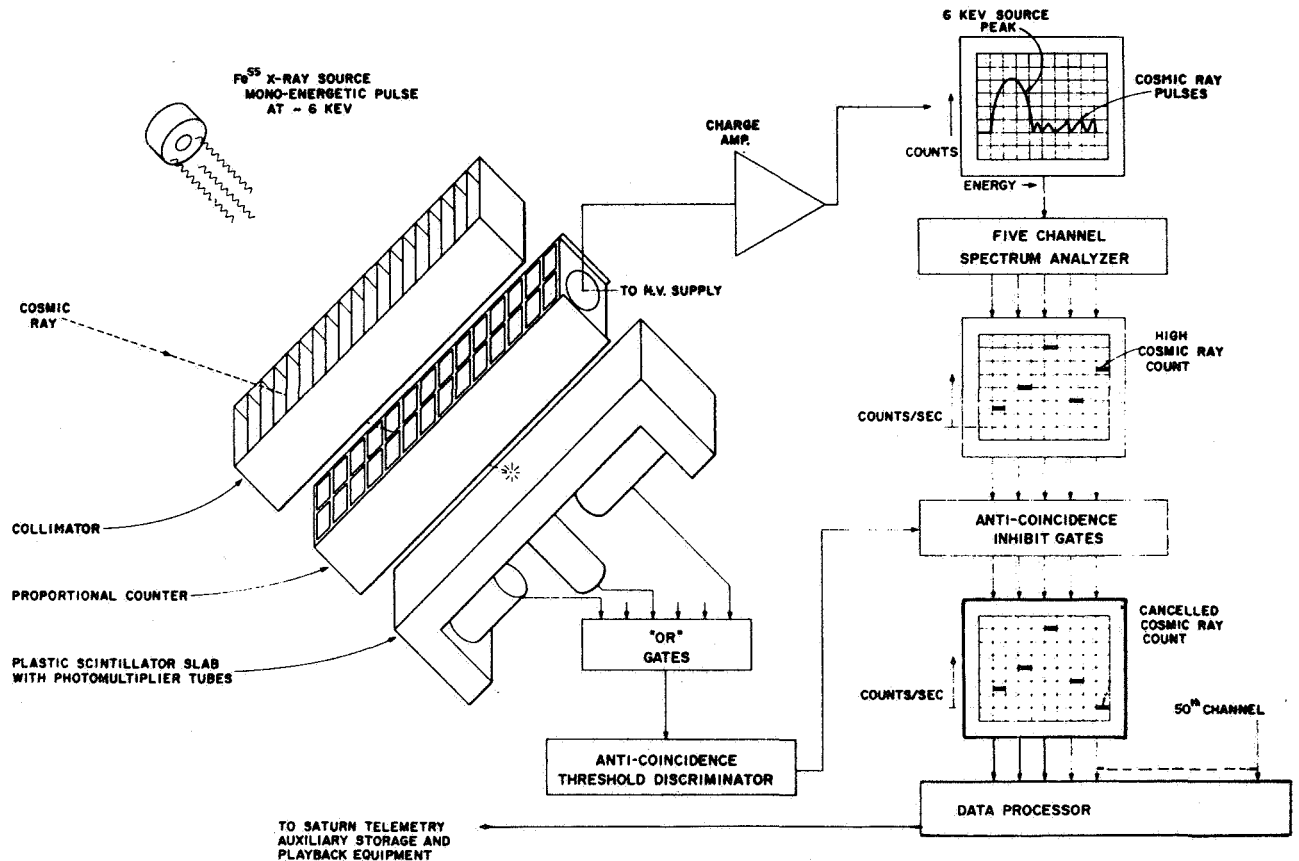


FIGURE 12. X-RAY PULSE ANALYSIS

modified by the effect of anti-coincidence counts of the fluorguard. The latter are the cosmic ray counts that have not been recorded. The output from each of these binary accumulators is then read into the Instrument Unit's pulse code modulator (PCM) system. Accumulation time for each register is 1 second. A read-in accumulation time of 1 second corresponds to a vehicle attitude change of approximately 0.06 degree, which allows for obtaining angular resolutions.

The star trackers use an optical slit, photomultiplier system as shown in Figure 13. Each sensor consists of a slit collimator, focusing lens, photomultiplier tube, and nonreflective surface coatings. The slit collimator has a projected view of 20 degrees by 0.2 degree on the celestial sphere. The collimator slits are orthogonal to each other in their projection and are aligned parallel to the 45 degree collimator fins.

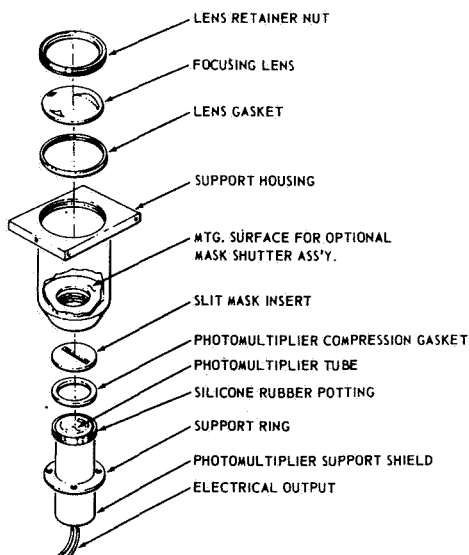


FIGURE 13. STAR TRACKER ASSEMBLY

Figure 14 shows the star tracker's projection in relation to the collimator's field of view. The star sensor outputs are processed with a time resolution equal to that of the counters and are presented in analog form to a signal conditioner. These data can be related directly to the IU computer clock time, to real time, and also to vehicle attitude and orbital position. In this manner the location of stars that pass through the proportional counters' scan field can be established. The wide dynamic

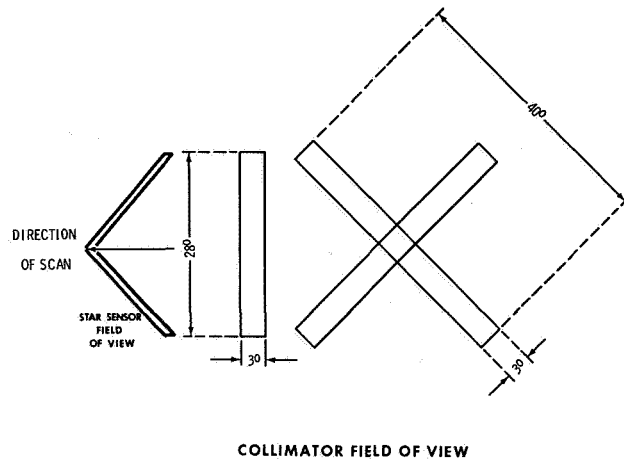


FIGURE 14. STAR SENSOR FIELD OF VIEW RELATED TO THE COLLIMATOR FIELD OF VIEW

sensitivity of the star sensors will provide backup data for identification of detected X-ray sources. The primary source of data for orientation and position determination will be the Saturn guidance and control system that operates through orientation information stored in the Instrument Unit's computer.

The auxiliary storage and playback (ASAP) unit is a data storage unit developed by the Astrionics Laboratory specifically for the S-027 experiment. The experiment package will perform signal conditioning and multiplexing of X-ray data. The digital data will be transferred to the Instrument Unit's telemetry system. The ASAP unit will be used to record experiment data from the IU, and upon command, the data will be transmitted to ground stations. The ASAP unit will also supply the experiment data processor with vehicle time and synchronization pulses. The ASAP unit has the capability of recording for 90 min so that it can be read out once per orbit. The readout can take place in less than 5 min.

RADIATION DETECTION PROCEDURE

The experiment package will be attached to a controlled temperature plate in a Saturn IB Instrument Unit (Fig. 15).

The attachment will be made by means of a support and deployment mechanism being designed and constructed by MSFC. After the primary mission of the Saturn booster vehicle is completed, the

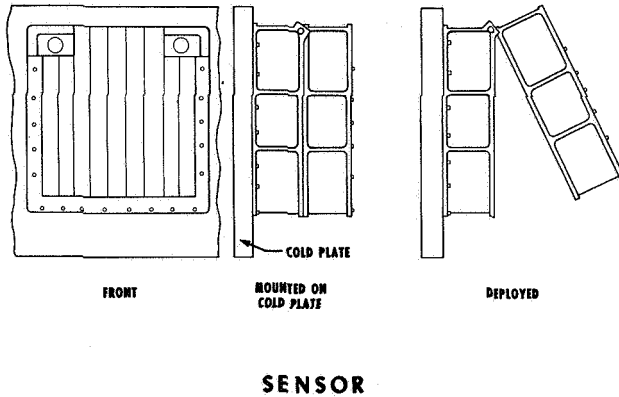
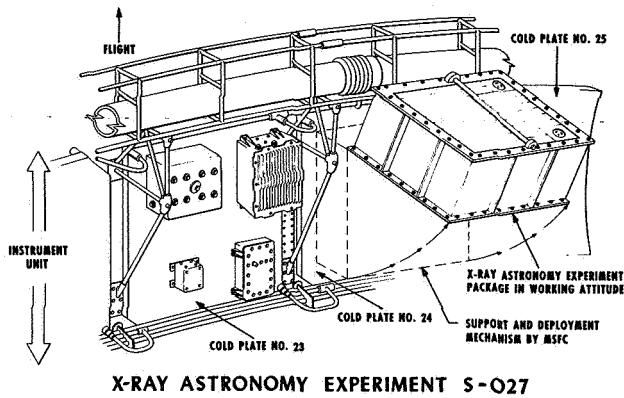


FIGURE 15. SENSOR PACKAGE ON A CONTROLLED TEMPERATURE PLATE

X-ray Astronomy Experiment will be deployed at an angle of 62.5 degrees with the top surface of the mounting bracket.

The S-IVB stage will be flight-vector oriented and rolled about the longitudinal axis so that the experiment's cold plate is parallel and adjacent to the surface of the earth.

In this position the sensor will scan a circular band of the sky approximately 28 degrees wide at a rate of 4 degrees per min (Fig. 16). The corresponding minimum detectable flux should be about one order of magnitude smaller than that which has been measured up to now by sounding-rocket-borne experiments. On the second orbit the S-IVB will be rolled through 45 degrees about its longitudinal axis to scan a second great-circle band. On the third orbit the S-IVB will be rolled in the opposite direction back through the first orbit position to an angle of -45 degrees and a third great circle will be scanned (Fig 17).

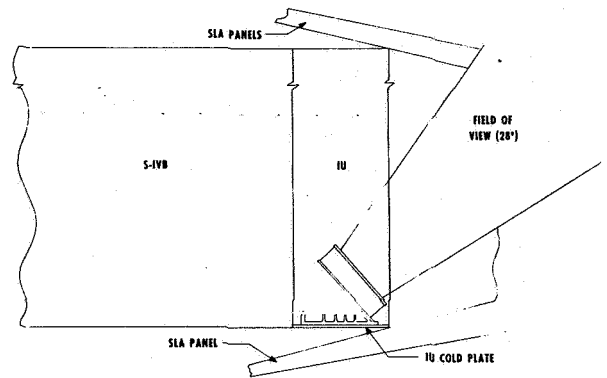


FIGURE 16. S-027 EXPERIMENT VIEW ANGLE

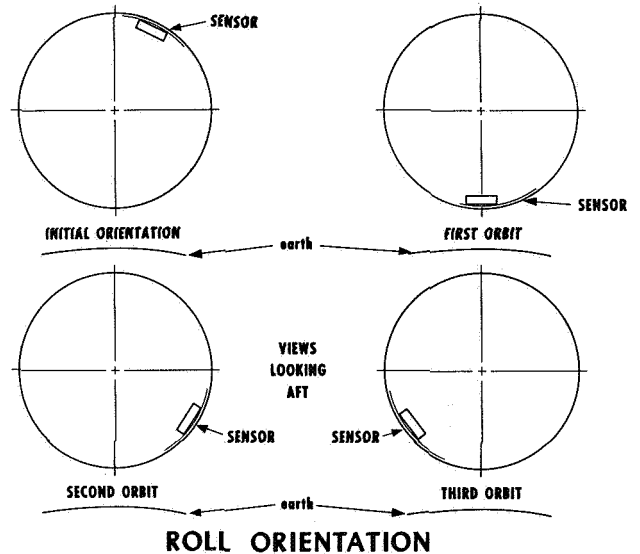


FIGURE 17. S-027 EXPERIMENT ORIENTATION ON THE SCANNING ORBITS

The pulse height analysis system will be calibrated periodically in flight. This will be accomplished by exposing each proportional counter to a 10 mCi Fe^{55} X-ray source. The ten sources are to be deposited on a rod directly above the proportional counter window. When not in the calibrate mode, the rod will be turned so that the sources look away from the counter.

During the altitude-controlled life of the S-IVB/IU stage, the X-ray detectors will scan a large cross-sectional area, about one half of the sky, thereby mapping the X-ray characteristics of galactic space.

There are two basic reasons for selecting a piggy back ride on the Saturn Instrument Unit. First, the normal stabilization mode of the S-IVB/IU in the parking orbit (probably about 100 n. mi.) provides approximately 4.5 hrs of sky survey per flight. This is significantly greater than that available from sounding rockets that have a flight time of 5 min. Second, the cost of performing the survey is minimized because the ride is free. Still another significant advantage is that the instrument carrier is flight programmed to maintain the flight vector parallel to the earth at all times. This advantage is realized in scan type experiments in allowing the transducer to be fixed in pointing direction relative to the orbit path, thereby sweeping out a complete great circle in space with one orbit.

CONCLUSION

This experiment is one of the approved Apollo Applications experiments and is assigned to the AAP I mission. It is desirable that this flight be followed by a second flight using the same detector to map the remaining half of the sky. These two flights will provide a comprehensive X-ray map of all sources on the celestial sphere with a flux one order of magnitude smaller than that which can be measured with sounding-rocket systems.

REFERENCES

1. Giacconi, R.; and Gursky, H.: Observation of X-Ray Sources Outside the Solar System. *Space Science Reviews* 4, 1965, pp. 151-175.
2. Freidman, H.: Cosmic X-Rays and Gamma Rays. *Astronautics and Aeronautics*, October 1965, pp. 8-12.
3. Kraushaar, William L.; and Scherb, Frank, (Principal Investigators): A Proposal to the National Aeronautics and Space Administration Marshall Space Flight Center for Development, Construction, and Flight of Survey-Type X-Ray Instruments to be Flown in the Saturn Instrument Unit. Department of Physics, College of Letters and Science, The University of Wisconsin, August 31, 1966.
4. Proposal to University of Wisconsin for a Saturn Launched X-Ray Astronomy Experiment. Space Craft Inc., SCI Proposal P66-309, August 10, 1966.

DEVELOPMENT OF AN AM BASEBAND TELEMETRY SYSTEM FOR WIDEBAND DATA

By
Frank Emens

INTRODUCTION

Over the past ten years the demand for telemetry channels with bandwidths suitable for transmission of wideband data, such as structural vibration, acoustics, and aerodynamics measurements, has far exceeded the capability of telemetry systems that existed at the beginning of the period.

Telemetry designers, in their effort to supply wideband channel capability to meet this demand, have concentrated their efforts in two areas: constant bandwidth FM (CBW-FM) and AM baseband techniques. Although there are some difficulties involved in its implementation, the concept of CBW-FM is a logical development from the proportional bandwidth FM telemetry technique that has been in wide use for many years.

In this paper the term "AM baseband" denotes a method of frequency division multiplexing which modulates a conventional FM telemetry transmitter by employing an array of amplitude modulated sub-carriers. The baseband spectrum is that band occupied by the subcarrier array. The AM subcarrier modulation might be conventional double sideband with carrier, as in AM broadcasting; double sideband suppressed carrier (DSB); or single sideband suppressed carrier (SSB), as used in telephone carrier multiplex systems. The suppressed carrier techniques, since they do not require the allocation of any of the transmission link's information handling capability to carrier signals, are the only ones considered here.

AM BASEBAND TELEMETRY SYSTEMS

Since 1958, the Telemetry Systems Branch, Instrumentation and Communication Division of Astrionics Laboratory, has been engaged in the study and development of AM baseband telemetry systems. The decision at MSFC to concentrate on the development of AM baseband techniques was based

largely on consideration of their superiority in terms of bandwidth utilization efficiency. Table I compares the RF bandwidth utilization efficiency of SSB, DSB, and CBW. RF bandwidth utilization efficiency is the ratio of total nominal channel bandwidth available in a frequency division multiplex to the RF bandwidth required to transmit the multiplex. In each case the number of channels and the spacing between channels is held constant and the channel bandwidth is varied according to the modulation technique. In regard to FM techniques, the term D_f is the deviation ratio,

defined as the ratio of peak frequency deviation to the maximum modulating frequency. Other assumptions used in making this comparison are the use of (1) a 100 kHz baseband, (2) a peak carrier deviation of ± 125 kHz, and (3) the approximation that the bandwidth of an FM carrier modulated by a complex signal is two times the sum of the peak carrier deviation and the highest modulation frequency.

TABLE I. COMPARISON OF RF BANDWIDTH UTILIZATION EFFICIENCY

CARRIER	% UTILIZATION
SSB/FM	10.7%
DSB/FM	5.1%
CBW FM/FM	
$D_f = 1$	4.9%
$D_f = 2$	2.5%
$D_f = 3$	1.6%
$D_f = 4$	1.2%
$D_f = 5$	1.0%
NOTE: D_f is deviation ratio.	

The bandwidth utilization efficiencies for DSB and CBW are almost identical when the CBW channel is operating with a deviation ratio of 1. In practice, operation at this low deviation ratio can result in increased distortion from sideband attenuation.

Also, since it is practical to use automatic deviation control with AM subcarrier techniques, a DSB subcarrier can enjoy an advantage of several decibels in signal-to-noise ratio over the equivalent FM subcarrier. Figure 1 shows the tradeoff relationship between signal-to-noise ratio and data bandwidth for an FM subcarrier as the deviation ratio is varied. The curve for DSB and SSB shows the signal-to-noise performance of an AM baseband subcarrier as compared to equivalent FM subcarriers. Each curve is normalized to the performance of an FM subcarrier with a deviation ratio of 5. The advantage gained by employing automatic gain control is a function of the factor C_s/L , which for the DSB/SSB curve is equal to 4. C_s is the crest function of the input data and L is the load factor of the system or, in other terms, the ratio of the instantaneous system loading to the full load condition. The value of 4 for C_s/L can exist when $C_s = 4$, which is the case for gaussian data, and $L = 1$, which is the full load condition.

In 1958, when preliminary studies of measuring requirements for a generation of large launch vehicles were begun, it became apparent that no telemetry technique existed that would accommodate the need for vibration telemetry channels. Because of the rather obvious advantages of the AM baseband techniques, a study was undertaken to see if they could be used for telemetry systems. After an extensive survey of the literature describing such techniques as implemented for telephone carrier multiplex applications, an approach was formulated that appeared to be feasible. Before this approach could be implemented in a form suitable for space applications, it was necessary to do considerable development in the area of carrier synthesis and filter design.

The filter development required extensive adaptation of the electromechanical filter design used in military communications equipment. This filter uses an array of precisely ground metal discs that are shaped to be mechanically resonant at frequencies in the vicinity of 455 kHz (Fig. 2). Each

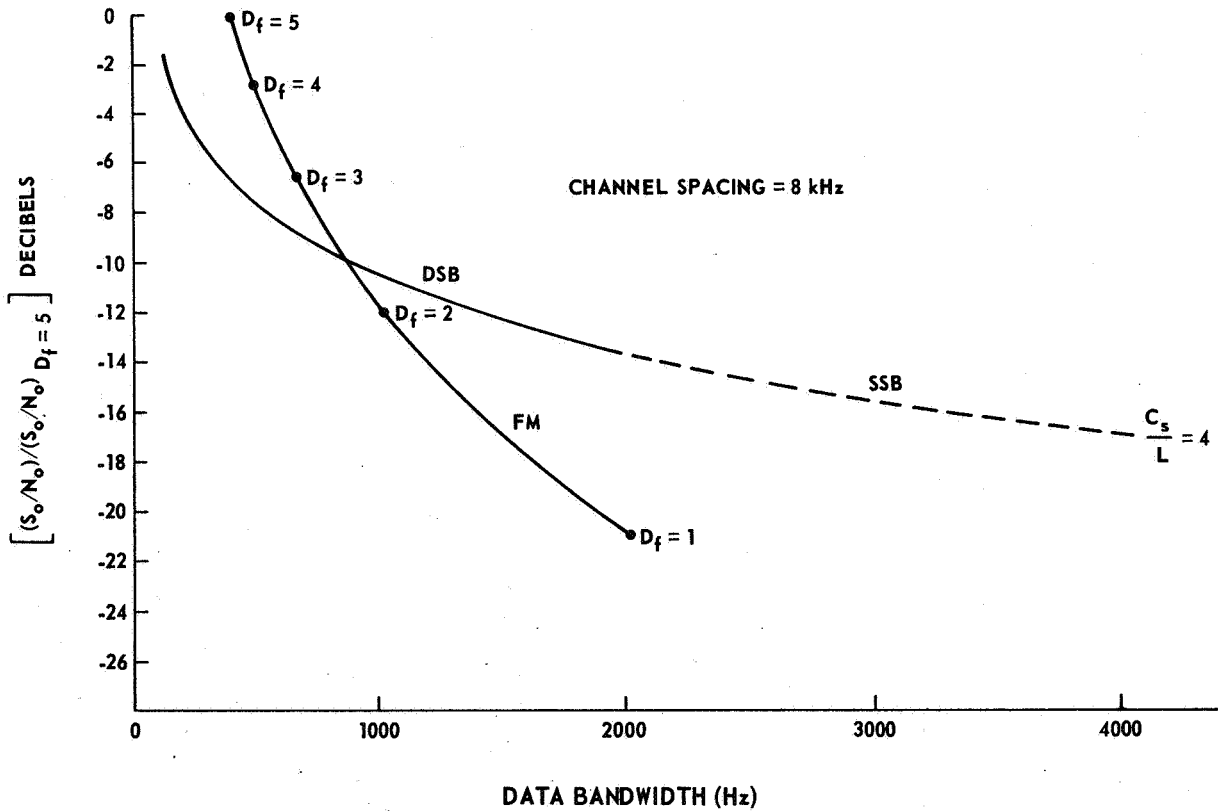


FIGURE 1. CHANNEL RESPONSE VERSUS SIGNAL/NOISE RATIO FOR A GIVEN CHANNEL LOCATION

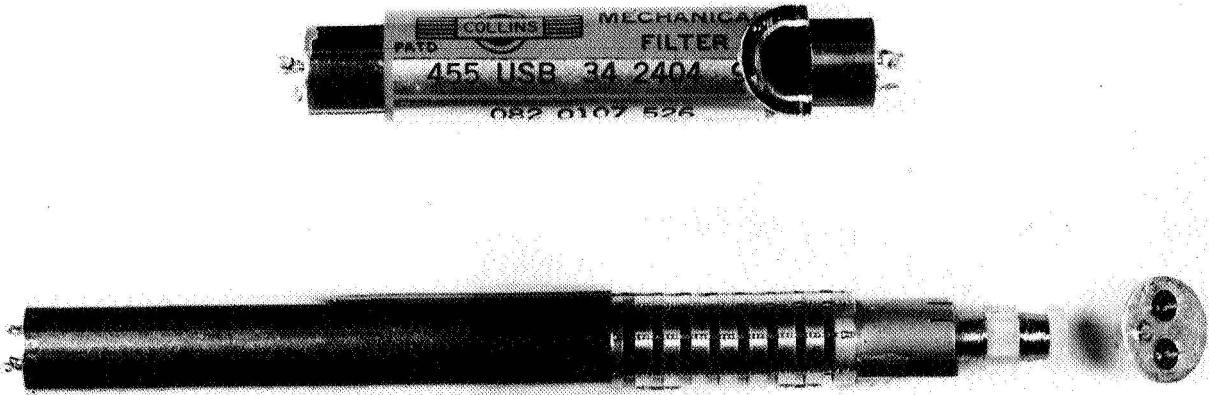


FIGURE 2. ELECTROMECHANICAL BANDPASS FILTER FOR SATURN SS-FM TELEMETRY SYSTEM

disc acts as the mechanical equivalent of a high Q , single tuned, resonant circuit. If the resonant frequencies of the discs are properly selected, and if they are intercoupled in the proper way, the resulting array will act as the mechanical equivalent of a complex filter network.

Electromechanical transducers are employed at each end of the array to excite the array with an electrical input signal and to produce an electrical output signal. To make the filter perform satisfactorily when subjected to the vibration environment encountered on a launch vehicle, it was necessary to develop a new transducer technique using magnetostrictive ferrite rods and to develop new techniques for coupling the discs together. The telemetry system that resulted from this development could accommodate 15 channels of data with a frequency response from 30 Hz to 3 kHz on one RF link. The subcarrier modulation technique used was SSB. The system was completed in time for the second Saturn I flight in 1961. (Fig. 3). With minor design changes, the same system has since been used on all research and development stages in the Saturn program. It is estimated that more than 1,000 vibration measurements have been made with the system.

The Saturn SS-FM system is not without faults. Since the modulation technique used is SSB, the channel frequency response cannot be extended to dc. The phase response of the mechanical filters used for sideband selection is quite nonlinear and the amplitude response across the channel passband is not uniform. This, in addition to phase ambiguities introduced in the frequency synthesis process, makes the system unsatisfactory for measurements that

require accurate waveform reproduction. Although the phase errors introduced by the system prevent its use for waveform reproduction, they do not affect the validity of the data for power spectral density analysis. Since, until recently, the bulk of Saturn vibration measurements have been destined for power spectral density analysis, the SS-FM system has served satisfactorily.

The trend in recent years has been toward requirements for improved low-frequency response and waveform definition in vibration measurements. Two factors have been responsible for the change in emphasis: more sophisticated measurements are required, especially in the field of unsteady aerodynamics measurements; and the increasing structural size of vehicles, especially the Saturn series, has lowered the range of vibration spectral components.

With present day technology it is practical to improve the characteristics of an SSB channel significantly over the performance of the Saturn system. The useful low-frequency response can be extended to 10 Hz; the phase response can be controlled, although it cannot be linearized; and the passband shape can be made uniform enough to make individual channel frequency response compensation unnecessary. A single sideband subcarrier channel is still limited, however, in that dc response cannot be achieved. Phase errors are induced in the data output of an SSB modulator-demodulator pair by failure to completely correct for the effect of tape recorder speed variations. These errors assume a form that is especially damaging to waveform reproduction.

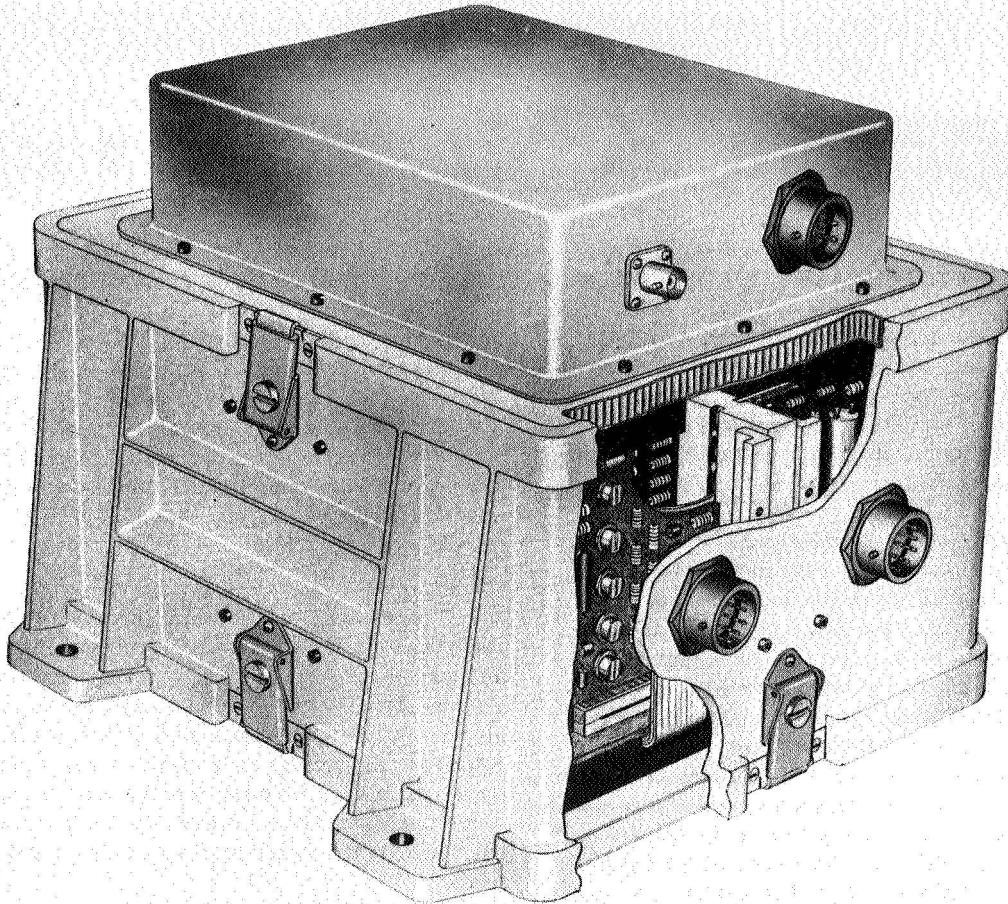


FIGURE 3. SATURN SS-FM TELEMETRY SYSTEM

It was decided, as a result of the previous disadvantages, that something other than SSB subcarriers was necessary for accurate waveform reproduction. The improved SSB subcarrier performance, however, was considered necessary as an improvement in the ability to transmit power spectral density data.

The characteristics required of a channel acceptable for accurate waveform reproduction and the channel fidelity desired in a new system are:

1. Low frequency response extending to dc.

2. A flat passband amplitude response curve or a curve that is simple enough and predictable enough to allow use of a single compensation curve for all channels.

3. Linear phase response.

4. Phase coherence between channels so that meaningful channel-to-channel phase correlation analysis may be performed.

Each of these requirements can be met by a double sideband channel. If the phase accuracy of the carrier reconstructed on the ground for demodulation purposes is adequate for good SSB performance, very little modification is needed to make a combination telemetry system practical. A combination system would allow the interchangeable use of SSB and DSB channels on a single RF link. The proper choice of channel carrier frequencies will also allow a user to interleave AM subcarrier and constant bandwidth FM subcarriers where the particular characteristics of FM are needed.

In 1965, a development program was started at MSFC with the goal of developing a highly flexible telemetry system for wideband data. The system would allow the intermixture of SSB, DSB, or FM, depending on the channel performance needed for each measurement. The user would have the option of using only alternate channel locations and doubling the upper frequency response limit where necessary. The channel location format to be used would place subcarrier frequencies at multiples of 4 kHz. The channel locations for current constant bandwidth FM systems are at multiples of 8 kHz. The compatibility of these formats is easily seen. Table II lists the nominal channel bandwidths available for SSB, DSB, and CBW-FM with different deviation ratios.

TABLE II. NOMINAL CHANNEL BANDWIDTHS

MODULATION FORMAT	CHANNEL SPACING		
	4 kHz	8 kHz	16 kHz
SSB	2.0 kHz	4.0 kHz	8.0 kHz
DSB	1.0	2.0	4.0
FM ₁	—	2.0	4.0
FM ₂	—	1.0	2.0
FM ₃	—	0.7	1.3
FM ₄	—	0.5	1.0
FM ₅	—	0.4	0.8

GENERATION OF DSB

Figure 4 is a much simplified block diagram of a DSB multiplexer. A channel of input data, which must be inherently band limited or which must be band limited by the input low-pass filter, is applied to a balanced modulator. The carrier signal applied to the modulator is selected to translate the input data

to its assigned location in the baseband spectrum. The output of the modulator is a double sideband pair centered about the carrier frequency. For this discussion it is assumed that an idealized implementation is used and no spurious modulation products are present. This output is combined with the outputs of several similar modulators, each with its unique carrier frequency, in a linear summing network. The output of the summing network is a frequency division multiplex signal that may be used to modulate a telemetry transmitter.

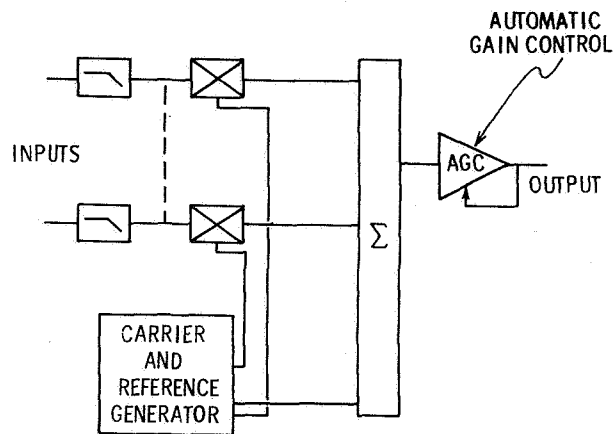


FIGURE 4. IDEALIZED DSB MULTIPLEXER

AUTOMATIC GAIN CONTROL

Some characteristics of a suppressed carrier AM subcarrier are as follows. The output amplitude of such a subcarrier is directly proportional to the amplitude of the modulating signal. If a telemetry transmitter is frequency modulated by the composite of several subcarriers, the transmitter deviation is a function of the total input data activity. If only one channel is active, or if all channels are active but only at a fraction of their full scale value, the transmitter deviation will be small compared to its level during full system activity. This represents an inefficient use of the transmitter's information capability.

If the composite multiplex signal (CMS) is applied to an automatic gain control (AGC) amplifier (Fig. 4), the transmitter deviation is maintained at the maximum allowed level over a wide range of input activity. If only a single channel is active, it will be allotted the full transmitter deviation, therefore undergoing an improvement in signal-to-noise over the configuration without AGC.

Since the gain of the AGC amplifier is a function of the composite data activity, which is not known at the receiving location, some information must be transmitted to enable the receiving demultiplexer to correct for the AGC action in the multiplexer. A constant amplitude reference signal, summed with the rest of the CMS and subjected to the gain variations of the AGC amplifier, will serve that purpose. Since the amplitude of the reference signal at the input of the AGC circuit is held constant, its amplitude at the output of the AGC circuit at any instant of time must be proportional to the instantaneous gain of the AGC amplifier at that time.

CARRIER SYNTHESIS

In demodulation of a suppressed carrier AM subcarrier signal, it is essential that the demodulation carriers be identical in frequency and phase with the suppressed subcarrier with negligible phase error. A technique exists for reconstructing demodulation carriers from the information inherent in the sidebands of a DSB signal. This technique, however, is only applicable to a DSB signal and cannot be made to operate with an SSB subcarrier. Since a telemetry system with capability both for DSB and SSB is needed, it is necessary to use another technique for reconstructing carriers.

The technique used requires that all of the modulation carriers used in the multiplexer, along with a reference signal that falls within the baseband, be derived from a single source in such a way that a precisely known frequency and phase relationship exists between the reference signal and each carrier. From the reference signal the carrier synthesizer can, using the precisely known relationships, reconstruct the full array of demodulation carriers. If precautions are taken to insure that AGC action does not reduce the level of the amplitude reference signal below the minimum level for satisfactory recovery of the carrier frequency and phase information, the same reference signal may be used to convey information about carrier frequency and phase as well as the AGC amplifier's instantaneous gain. This reference signal is commonly referred to as a pilot.

DEMODULATION OF DSB

The demultiplexing and demodulation of an array of DSB subcarriers is, to a large degree, a reversal of the processes used in generating the array.

Figure 5 is an idealized block diagram of a demultiplexer for DSB channels. The composite

signal is acted upon by an AGC amplifier, which maintains the pilot signal at a constant level at the amplifier output. This is accomplished by separating the pilot signal from the composite signal in the reference detector block and using its amplitude to generate a feedback control signal for the AGC amplifier. If the demultiplexer AGC circuit succeeds in maintaining the pilot at a constant amplitude, its gain variations exactly complement the gain variations taking place in the multiplexer AGC amplifier as it compensates for variations in data activity. If the two gain variations are complementary, the AGC action is completely compensated for and the original relative amplitude of each subcarrier in the composite is restored.

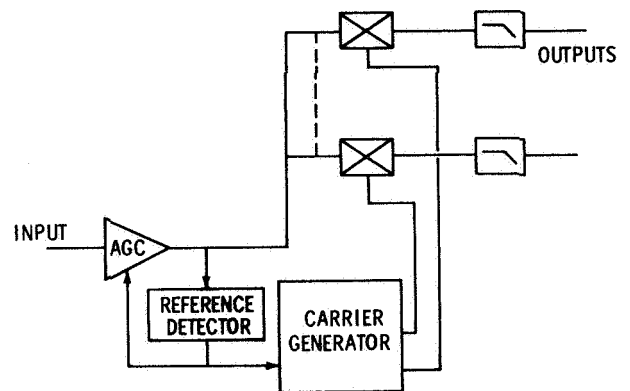


FIGURE 5. IDEALIZED DSB DEMULTIPLEXER

The reference detector block also derives accurate phase and frequency information from the pilot and supplies it to the carrier generator. The carrier generator uses that information to reconstruct the coherent carriers needed for demodulation.

The composite signal appearing at the output of the AGC amplifier is applied to a group of balanced modulators, each of which is also driven by an appropriate carrier frequency. At the output of each modulator appears the data for the channel selected by the carrier and an undesired modulation product at twice the carrier frequency. A low-pass filter separates the desired data so that it can be amplified and available as an output signal.

SQUARE WAVE MODULATORS

Figures 4 and 5 are quite drastically simplified and idealized. A brief discussion follows of two of the disparities between the ideal situation and the

actual implementation of suppressed carrier AM techniques.

It was assumed in the system descriptions that ideal modulators were used. If such modulators existed, no channel filtering would be necessary other than the optional input low-pass filter before the modulator and the low-pass filter required at the output of the demodulator. Since these filters both operate at the untranslated data frequency, the same filter design can be used for each channel. If this is done, almost no difficulty is encountered in matching the phase and frequency response curves of different channels.

Ideal modulators are not readily available for the frequency range of interest and the more conventional "chopper" modulator must be used. The effect of using a chopper modulator is identical to that of using a square-wave carrier signal with an ideal modulator. If a square-wave carrier is applied to a balanced modulator, the output will contain modulation products at odd harmonics of the carrier frequency. If the balanced modulator is functioning as a demodulator, the output will contain spurious responses to signals located at harmonics of the carrier. The impact of this problem on system design is a requirement for filters located at the modulator outputs in a multiplexer and filters at the demodulator inputs in a demultiplexer. The post-modulation filter removes the harmonic product that would otherwise interfere with other channels in the baseband. The pre-demodulation filter eliminates the harmonically related channels in the baseband that would otherwise be demodulated and appear as interfering data.

Since each of these filters must operate at a different frequency within the baseband, each filter is a different design problem. The problem of maintaining equivalent frequency response, phase linearity, and group delay for each channel is thus made much greater than it would be if ideal modulators were available.

TAPE SPEED FLUCTUATIONS

In almost any operational application of a telemetry system, it is necessary to record the baseband signal on some form of magnetic tape recorder for playback at a later time. Any practical tape recorder can be expected to degrade the baseband composite signal because of its short term speed variations, commonly described as flutter or dynamic-time-base errors. The effect of these time-base variations is a continuously varying shift in the frequency of

every component. The shift is, for every component, proportional to the nominal frequency of that component.

In designing a frequency division multiplex system using suppressed carrier AM techniques, particular attention must be devoted to the methods used in reconstructing the carriers for demodulation. Techniques must be used which insure that the frequency deviations of the reconstructed carriers match as closely as possible the deviations imposed by the tape recorder on the subcarrier signals. Since the tape recorder affects the pilot signal just as it does the subcarrier, the tape recorder error information is superimposed on the pilot signal and can be used by the carrier generation circuitry to compensate the errors.

If a demultiplexer is to compensate adequately for these time-base perturbations, the following major points must be met:

1. The filter used to extract the pilot signal from the composite signal must be narrow enough to minimize interference from adjacent channels and baseband noise, yet be wide enough to minimize degradation of the tape speed error information.

2. The filter must have a phase response characteristic that is linear over the range of deviation expected in the pilot signal. These conflicting requirements can be met most effectively by a higher-order phase-locked loop.

3. The frequency synthesis techniques used to generate demodulation carriers must be selected to insure that the frequency deviations appear on each carrier signal with the proper sign and amplitude.

4. In a demultiplexer the subcarrier information and the carrier information arrive at the demodulator by different paths. The subcarrier information goes through a channel separation filter and through one or more baseband amplifiers before reaching the demodulator. The carrier information goes through the pilot selection filter and through the carrier synthesis circuitry to reach the demodulator. If the time required for transit through these two entirely different signal paths is not exactly matched, the frequency deviation imposed on the carrier by tape speed error will not be coherent with the deviations imposed on the subcarrier, and an error is introduced in the demodulated signal.

CONCLUSIONS

It has been demonstrated that carrier synthesis and reconstruction techniques do exist that can, in a practical implementation, provide the necessary degree of phase coherence.

A single channel DSB breadboard has been constructed. It was shown that the degree of accuracy required for a telemetry application can be achieved even though the complex is perturbed by a tape recorder.

Breadboards of a multichannel multiplexer and a matching multichannel demultiplexer have been designed and are available at MSFC for detailed testing.

FUTURE PLANS

It was necessary that the multiplexer and demultiplexer breadboards be designed and built by different contractors. Although our definition of the baseband and the interface between the two units was as detailed as possible, some effort will be required to resolve areas of incompatibility between units.

Then it will be necessary to select critical parameters in the carrier reconstruction loops and in the AGC area. Both of these areas have been covered in some detail analytically, but the final parameter selection will be the result of experimentation.

An obvious implication of the difficulties caused by the need for square wave modulation is that some effort should be made toward development of an ideal modulator, or something approaching the ideal. In support of the development effort for AM baseband systems, MSFC has been pursuing study and development programs aimed toward perfecting the true product modulator (an ideal balanced modulator).

Several implementation techniques are being investigated, the Hall Effect and Quarter Square multiplier being representative. At present, none of the techniques will perform over the required frequency range and none will withstand a space flight environment. The investigations, however, will be continued.

Data from breadboard testing combined with analyses of information obtained from the development effort will be used to design and construct operational hardware that can be used to meet expanding requirements for wideband data.

REDUNDANCY REMOVAL TECHNIQUES FOR COMPRESSION OF TELEMETRY DATA

By

Gabriel R. Wallace

SUMMARY

This paper describes some of the achievements and consequent benefits gained by MSFC during the years of investigation of redundancy removal techniques. Results of both analytical and empirical studies of various phases of redundancy removal techniques are reported. Redundancy removal occurs after encoding the data but prior to transmission, with the exception of reconstruction techniques (which obviously concerns post transmission operations). This paper lists the basic findings and assumptions in the area of redundancy removal and then discusses the chronological development of the program.

INTRODUCTION

The requirement for redundancy removal is evident upon analyzing the probable frequency content of normal pulse code modulation (PCM) data. If the data to be transmitted have the power density spectrum outline shown in Figure 1, sampling theory yields an adequate rate of $1/2f_c$. However, this is an ideal situation. Actual cases are typified by the spectrums shown in Figures 2 and 3. For these situations,

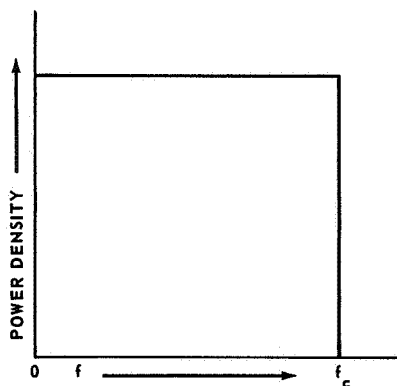


FIGURE 1. REPRESENTATIVE DATA SPECTRA
($1/2f_c$ rate)

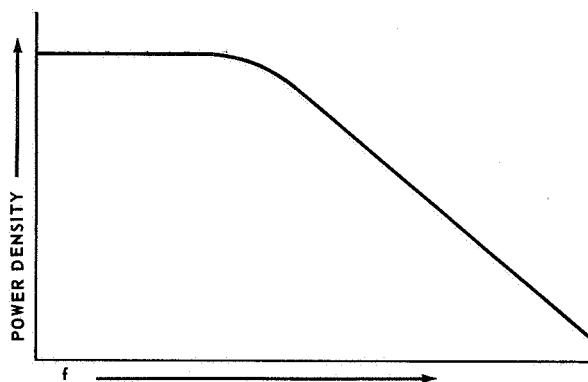


FIGURE 2. REPRESENTATIVE DATA SPECTRA
(Actual Rate)

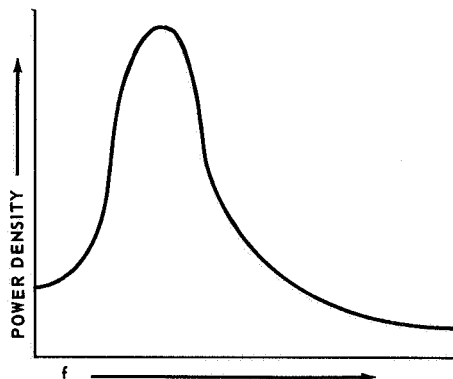


FIGURE 3. REPRESENTATIVE DATA SPECTRA
(Actual Rate)

a precise sampling rate is difficult to establish since data degradation could result from some frequency components being lost. On the other hand, the tendency to over-sample produces a high redundancy content in most transmitted messages.

To describe various aspects of inflight redundancy removal, two terms will be used: redundancy removal and data compression. In this paper these two terms are interchangeable and mean simply the

removal of redundant information from an encoded message by some selective process.

INFLIGHT REDUNDANCY REMOVAL

ALGORITHM NOTATION

To refer to a particular method or redundancy removal technique, a shorthand notation of three letters denotes a particular redundancy removal algorithm.

Redundancy, the nonsignificant changes between adjacent data samples or among several samples, appears in nearly all data transmissions. To remove redundancy it is necessary to monitor some parameter of the data that is proportional to the change. A particular derivative is usually selected; the order associated with a given method of redundancy removal is simply the order of this derivative and is limited by implementation feasibility to either zero (Z), first (F), or second (S) order derivatives. The first letter (Z, F, or S) of the three letter notation denotes the order of the algorithm.

A corridor refers to the region in which subsequent samples must fall in order to be classified as redundant. If, when once established, the width of the corridor remains constant until a sample is classified as nonredundant, the corridor is said to be fixed (F). If, to the contrary, the corridor changes in width between the occurrence of nonredundant samples, it is said to be variable (V). The behavior of the corridor width is denoted by the second letter (F or V) of the three letter algorithm notation.

Finally, redundancy removal methods differ in the choice of the sample that is transmitted when a nonredundant sample is detected. One of the three following choices is denoted by the third letter of the three letter algorithm notation.

1. The nonredundant sample (denoted by N).
2. The sample preceding the nonredundant sample (denoted by P).
3. The predicted value of the sample preceding the nonredundant sample (denoted by A).

Many types of redundancy removal could be formulated by making various combinations of the

particular orders of redundancy removal, types of corridor, and samples transmitted. However, only eight algorithms were selected for analysis because the other methods of redundancy removal either resulted in large error, led to wholly unacceptable results, or were equivalent to other schemes. The eight algorithm descriptions and graphs explained in the following section of this paper were taken almost verbatim from Reference 1.

ALGORITHM OPERATIONS

Intuitively, there are at least two straightforward methods to accomplish inflight redundancy removal: prediction and interpolation.

Predictors are based on a finite-difference technique that permits an n^{th} order polynomial to be passed through $n + 1$ data points. The polynomial is extrapolated one unit at a time, which produces a predicted data point.

Interpolators are based on all previous data points (back to the last transmitted sample). This averaging process checks samples with past data points to see that they fall inside a tolerance band. Thus the interpolators are more difficult to implement than are the predictors.

The eight types of redundancy removal algorithms and their graphs are listed according to the method of inflight redundancy removal.

1. PREDICTOR

Zero Order, Fixed Corridor, Nonredundant Sample Transmitted (ZFN).

Rules for redundancy removal are as follows:

- a. The occurrence of a nonredundant sample requires that a new corridor be established. Lines of zero slope are drawn through the end points of the tolerance range placed around the nonredundant sample.
- b. If a subsequent sample lies inside the corridor, it is a redundant sample and is discarded.
- c. If a subsequent sample lies outside the corridor, it is a nonredundant sample and is transmitted.

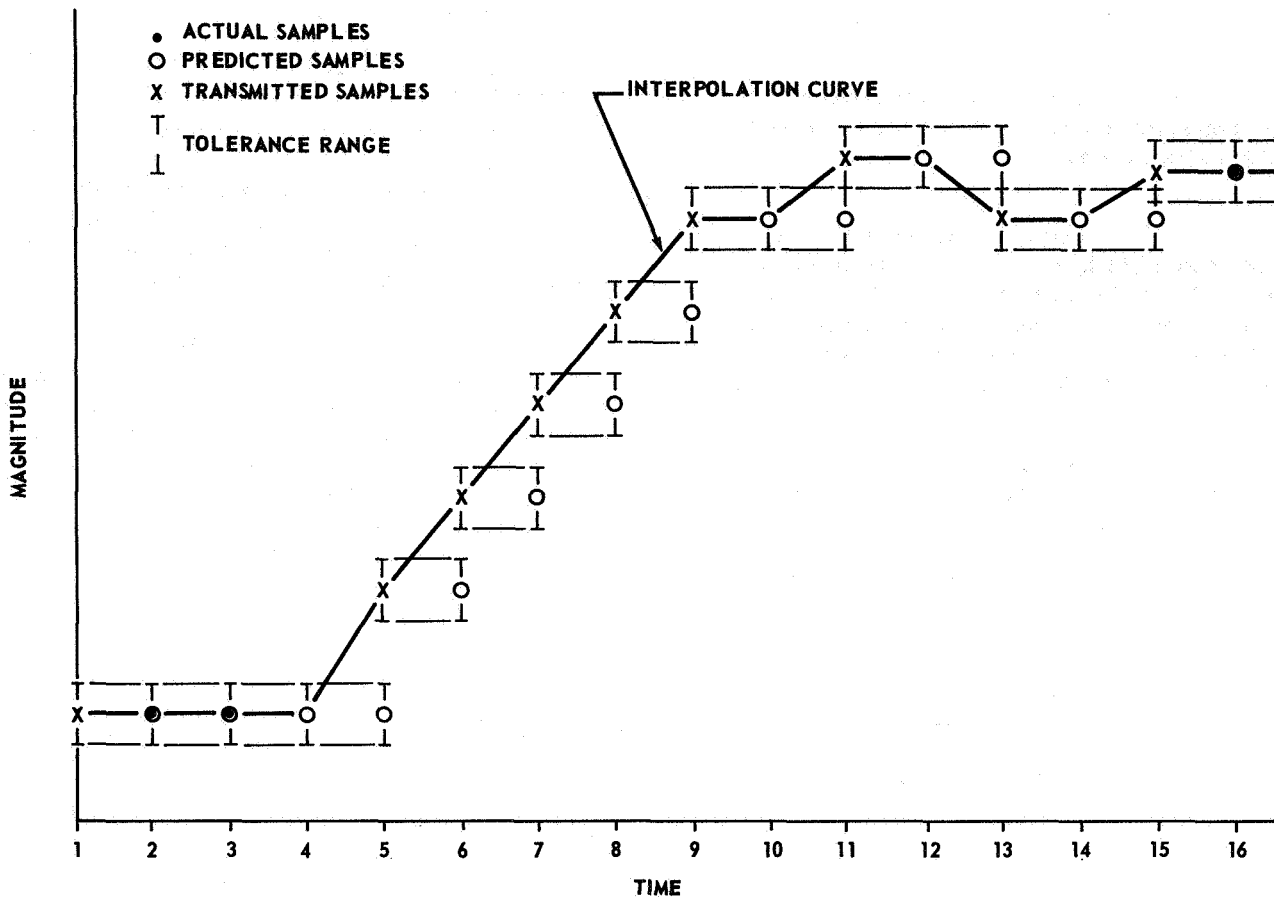


FIGURE 4. ZERO ORDER, FIXED CORRIDOR, NONREDUNDANT SAMPLE TRANSMITTED (ZFN)

Rules for reconstruction are as follows:

- a. If there are no omitted samples between transmitted samples, the latter is connected with a straight line.
- b. If there are intermediate omitted samples, a straight line of zero slope is drawn from the first transmitted sample to the time of occurrence of the sample preceding the second transmitted sample. The end of this line is then connected to the second transmitted sample with a second line.
- c. The maximum peak error between raw data and reconstructed, reduced data is plus or minus one-half tolerance range.

These rules are demonstrated in Figure 4.

2. INTERPOLATOR

Zero Order, Variable Corridor, Preceding Sample Transmitted (ZVP).

Rules for redundancy removal are as follows:

- a. The occurrence of a nonredundant sample requires that a new corridor be established. Lines of zero slope are drawn through the end points of the tolerance range placed around the nonredundant sample.
- b. If a subsequent sample lies inside the corridor, it is a redundant sample and is discarded. Each redundant sample modifies the corridor extended to the next sample in the following way. The new corridor consists of that part of the previous corridor which is overlapped by the tolerance range placed about the redundant sample.
- c. If a subsequent sample lies outside the corridor, it is a nonredundant sample, but it is not transmitted.

Rules for reconstruction are as follows:

a. If there are no omitted samples between two transmitted samples, the latter is connected with a straight line.

b. If there are intermediate omitted samples, a straight line of zero slope is drawn from the second transmitted sample back to the time of occurrence of the first sample following the first transmitted sample. The end of this line is then connected to the first transmitted sample with a second line.

c. The maximum peak error between the raw data and the reconstructed, processed data is plus or minus one-half tolerance range.

These rules are demonstrated in Figure 5.

3. INTERPOLATOR

Zero Order, Variable Corridor, Artificial Preceding Sample Transmitted (ZVA).

Rules for redundancy removal are as follows:

a. The occurrence of a nonredundant sample requires that a new corridor be established. Lines of zero slope are drawn through the end points of the tolerance range placed around the nonredundant sample.

b. A subsequent sample is redundant and can be discarded when one end of the tolerance range placed about the sample falls within the corridor. The sample itself is not required to be within the corridor. Each redundant sample modifies the corridor extended to the next sample in the following way. The new corridor consists of that part of the previous corridor that is overlapped by the tolerance range placed about the redundant sample.

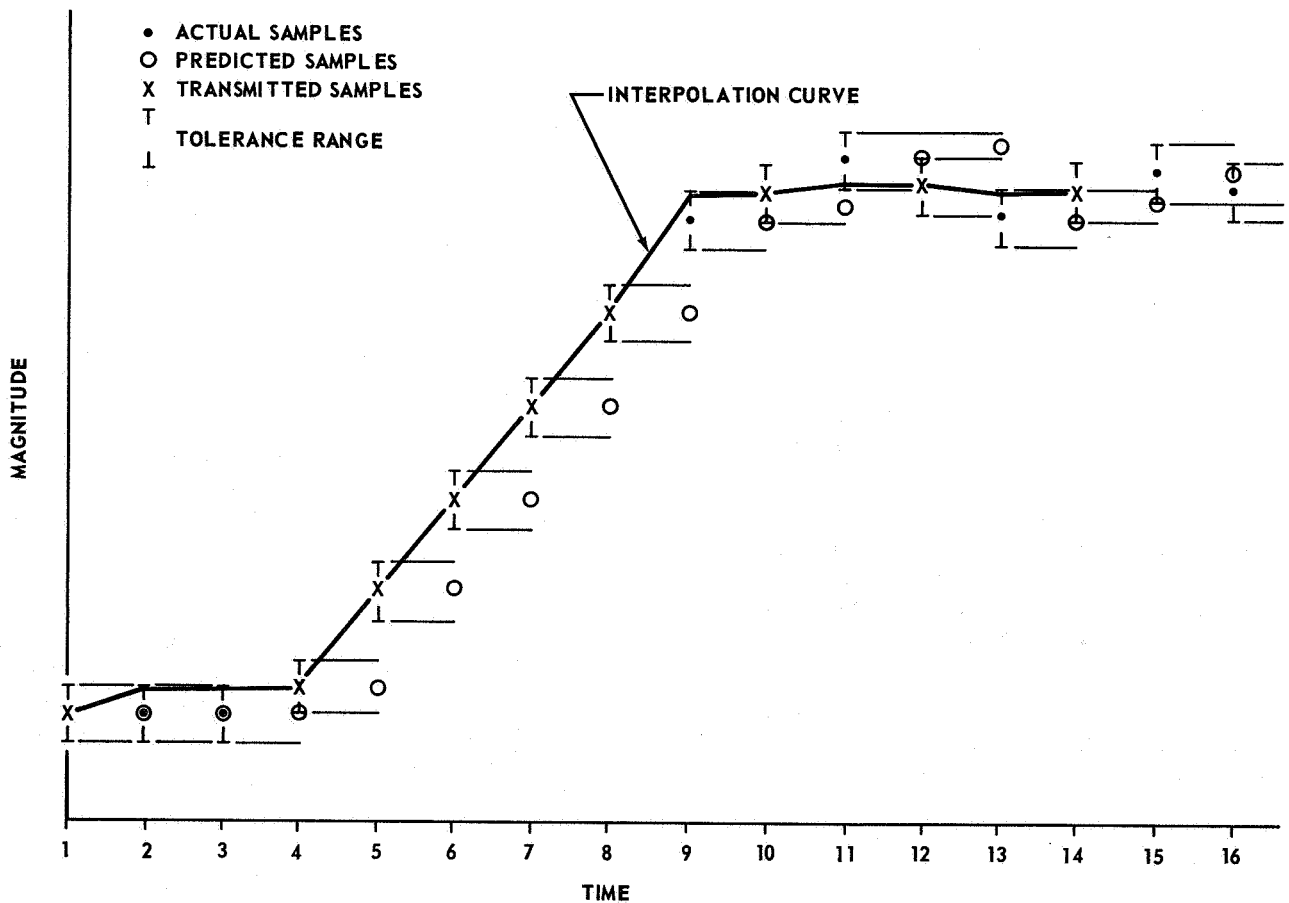


FIGURE 5. ZERO ORDER, VARIABLE CORRIDOR, PRECEDING SAMPLE TRANSMITTED (ZVP)

c. If the tolerance range placed about a sample does not overlap the corridor, the sample is nonredundant, but is not transmitted. Rather, the midpoint of the corridor used to analyze this sample, actually the predicted value of the sample, is transmitted for the preceding sample. Hence, the transmitted sample is not a real data sample but an artificial sample.

Rules for reconstruction are as follows:

- a. If there are no omitted samples between two transmitted samples, the latter is connected with a straight line.
- b. If there are intermediate omitted samples, a straight line of zero slope is drawn from the second transmitted sample back to the time of occurrence of the first sample following the first transmitted sample. The end of this line is then connected to the first transmitted sample.

c. The maximum peak error between the raw data and the reconstructed, processed data is plus or minus one-half tolerance range.

These rules are demonstrated in Figure 6.

4. PREDICTOR

First Order, Fixed Corridor, Nonredundant Sample Transmitted (FFN).

Rules for redundancy removal are as follows:

- a. The occurrence of a nonredundant sample requires that a new corridor be established. Tolerance ranges are placed around the nonredundant sample and the previous sample, and two straight lines are drawn, one line through the upper ends of the tolerance ranges and the other line through the lower ends.
- b. If a subsequent sample lies inside this corridor, it is a redundant sample.

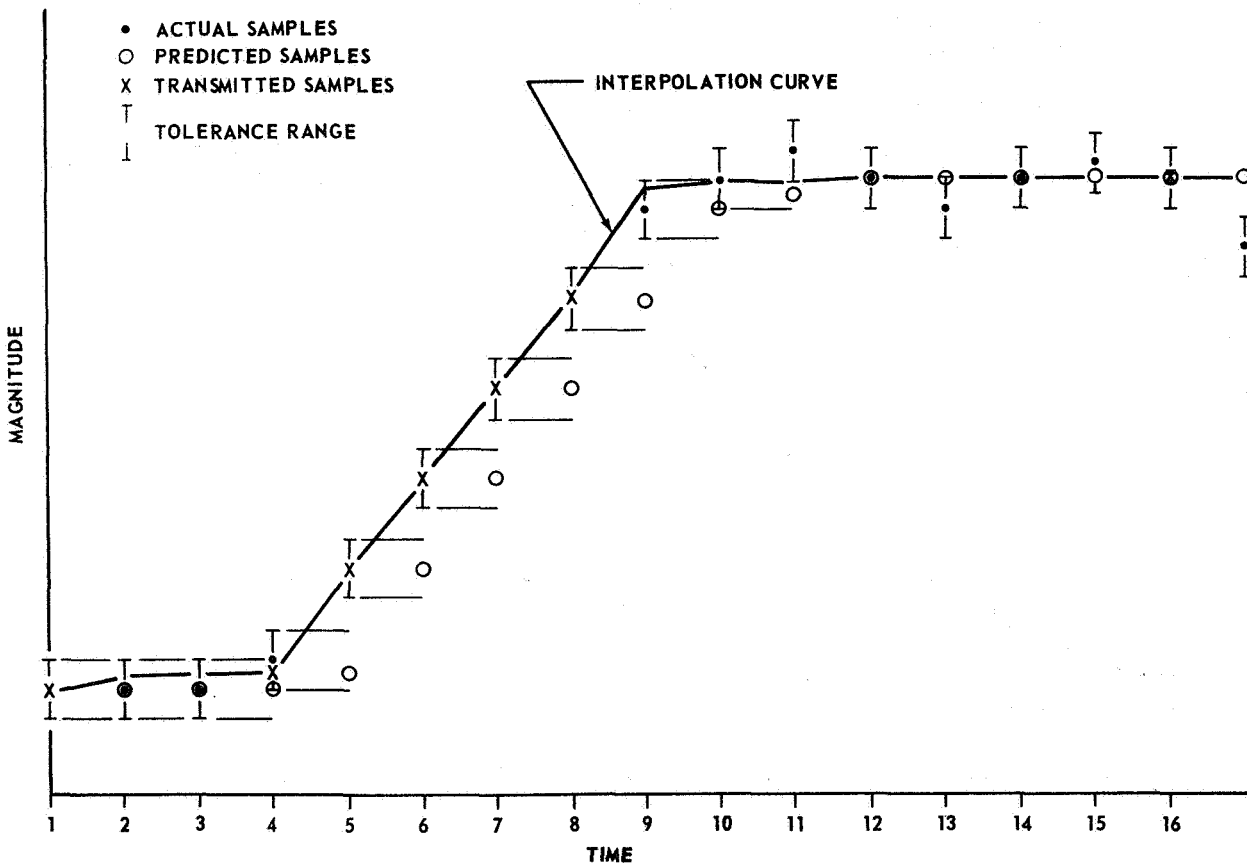


FIGURE 6. ZERO ORDER, VARIABLE CORRIDOR, ARTIFICIAL PRECEDING SAMPLE TRANSMITTED (ZVP)

c. If a subsequent sample lies outside the corridor, it is a nonredundant sample and is transmitted.

Rules for reconstruction are as follows:

- a. Transmitted samples are connected by straight lines.
- b. The maximum peak error between the raw data and the reconstructed, processed data approaches plus or minus full scale.

These rules are illustrated in Figure 7.

5. PREDICTOR

First Order, Fixed Corridor, Preceding Sample Transmitted (FFP).

Rules for redundancy removal are as follows:

a. The occurrence of a nonredundant sample requires that a new corridor be established. Tolerance ranges are placed around the nonredundant sample and the previous sample, and two straight lines are drawn, one line through the upper ends of the tolerance ranges and the other line through the lower ends.

b. If a subsequent sample lies inside this corridor, it is a redundant sample.

c. If a subsequent sample lies outside the corridor, it is a nonredundant sample, but it is not transmitted. Rather, the preceding sample is transmitted.

Rules for reconstruction are as follows:

- a. Transmitted samples are connected by straight lines.

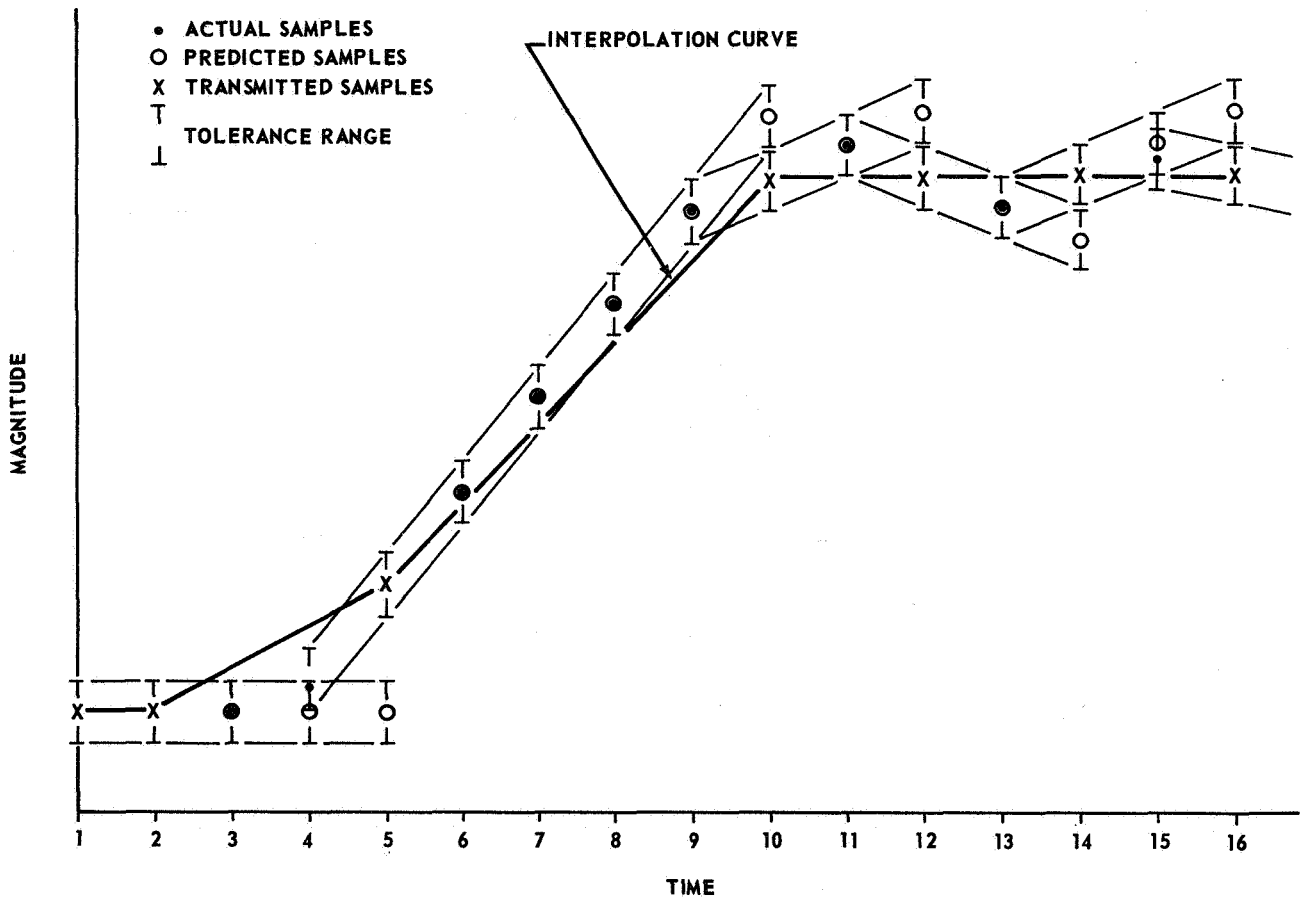


FIGURE 7. FIRST ORDER, FIXED CORRIDOR, NONREDUNDANT SAMPLE TRANSMITTED (FFN)

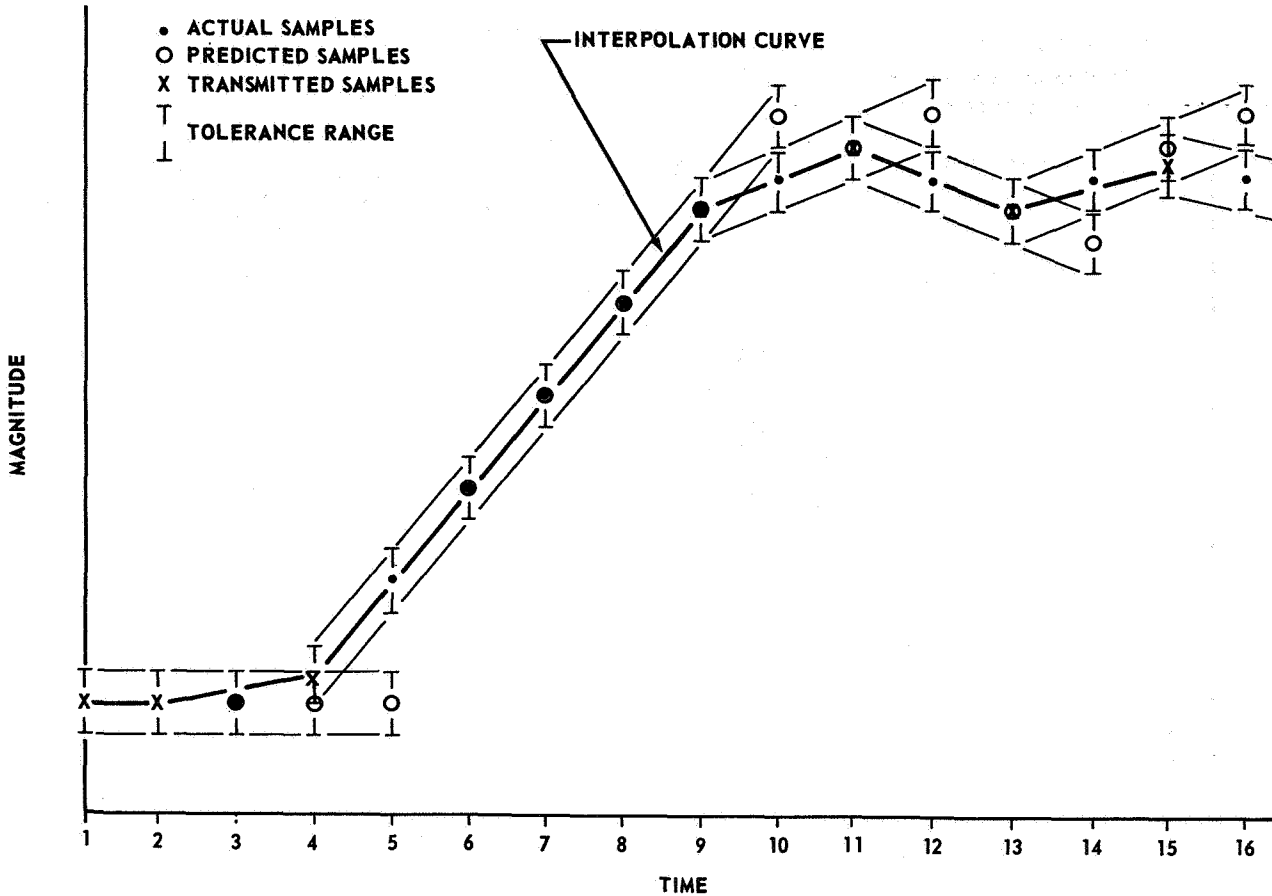


FIGURE 8. FIRST ORDER, FIXED CORRIDOR, PRECEDING SAMPLE TRANSMITTED (FFP)

b. The maximum peak error between the raw data and the reconstructed analyzed data approaches plus or minus one tolerance range.

These rules are illustrated in Figure 8.

6. PREDICTOR

First Order, Fixed Corridor, Artificial Preceding Sample Transmitted (FFA).

Rules for redundancy removal are as follows:

a. The occurrence of a nonredundant sample requires that a new corridor be established. Tolerance ranges are placed around the nonredundant sample and the artificial preceding sample that is transmitted. Two straight lines are drawn, one line through the upper ends of the tolerance ranges and the other through the lower ends.

b. If a subsequent sample lies inside this corridor, it is a redundant sample and is discarded.

c. If a subsequent sample lies outside the corridor, it is a nonredundant sample, but it is not transmitted. Rather, an artificial value for the previous sample is transmitted. This value is the midpoint of the corridor for the previous sample, which is the predicted value for that sample.

Rules for reconstruction are as follows:

a. Transmitted samples are connected by straight lines.

b. The maximum peak error between the raw data and the reconstructed, processed data is plus or minus one-half tolerance range.

These rules are illustrated in Figure 9.

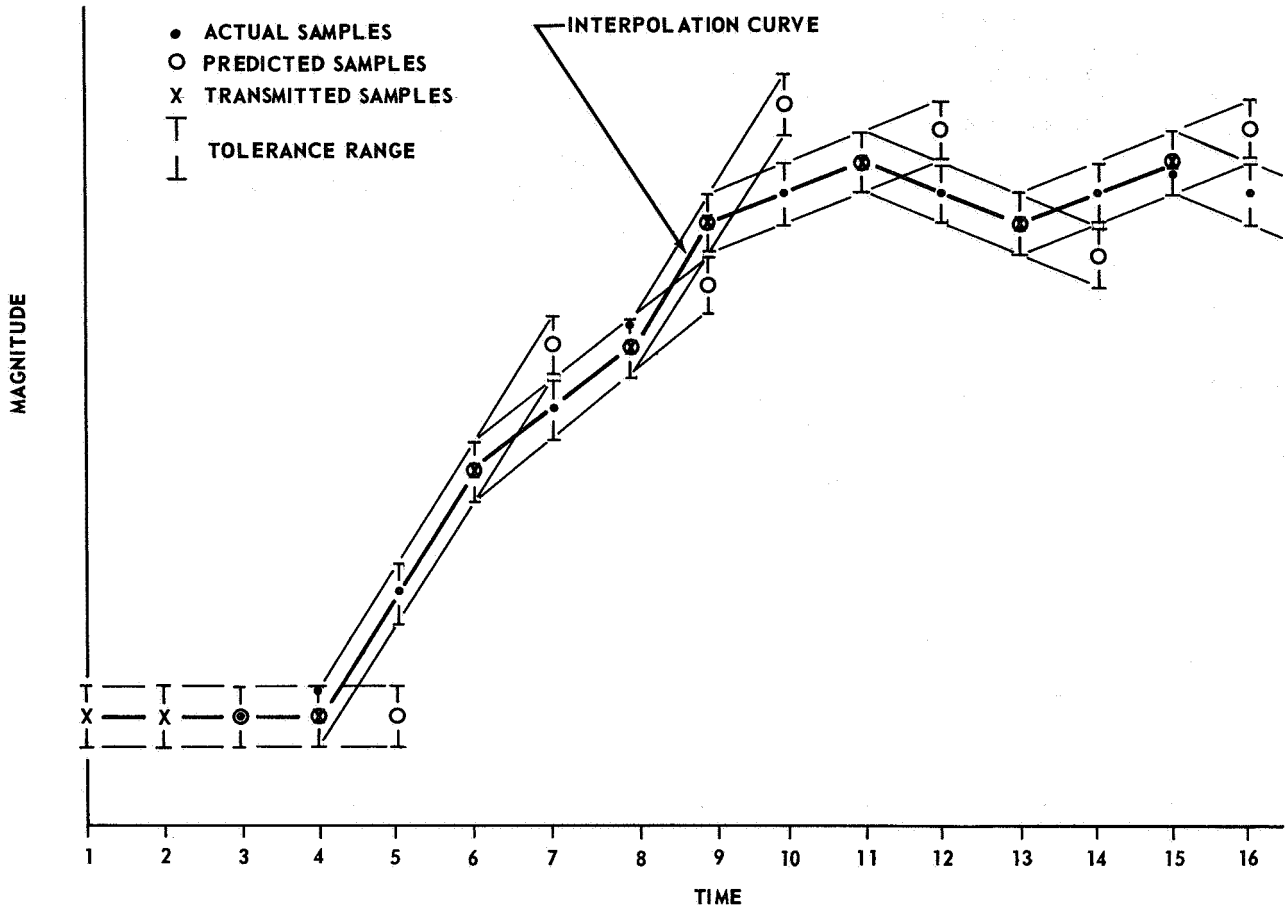


FIGURE 9. FIRST ORDER, FIXED CORRIDOR, ARTIFICIAL PRECEDING SAMPLE TRANSMITTED (FFA)

7. INTERPOLATOR

First Order, Variable Corridor; Preceding Sample Transmitted (FVP).

Rules for redundancy removal are as follows:

- a. The occurrence of a nonredundant sample requires that a new corridor be established. A tolerance range is placed around the nonredundant sample and two straight lines are drawn. The first line passes through the previous sample and the upper end of the tolerance range; the second line passes through the same sample and the lower end of the tolerance range.
- b. If a subsequent sample lies inside this corridor, it is a redundant sample and is discarded. Each redundant sample modifies the corridor extended to the next sample in the following way. If a boundary line of the corridor does not pass through the tolerance range placed around the redundant sample, a new

boundary is established that passes through the nearest end point of the tolerance range. Either or both boundary lines can be affected.

- c. A sample falling outside the corridor is a nonredundant sample, but it is not transmitted. Rather, the preceding sample is transmitted.

Rules for reconstruction are as follows:

- a. Transmitted samples are connected by straight lines.
- b. The maximum peak error between the raw data and the reconstructed analyzed data is plus or minus one-half tolerance range.

These rules are illustrated in Figure 10.

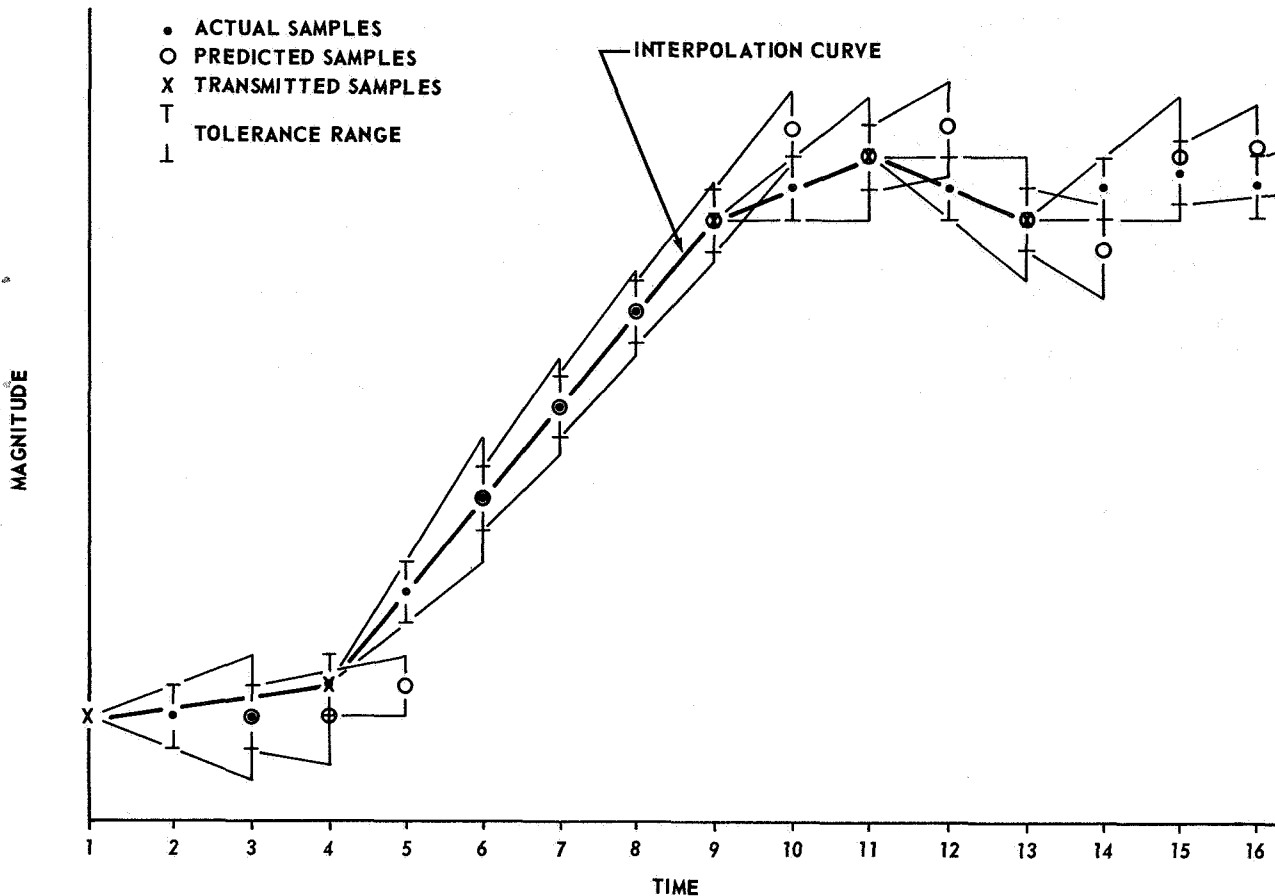


FIGURE 10. FIRST ORDER, VARIABLE CORRIDOR, PRECEDING SAMPLE TRANSMITTED (FVP)

8. INTERPOLATOR

First Order, Variable Corridor, Artificial Preceding Sample Transmitted (FVA).

Rules for redundancy removal are as follows:

a. The occurrence of a nonredundant sample requires that a new corridor be established. A tolerance range is placed around the nonredundant sample and two straight lines are drawn. The first line passes through the artificial preceding sample, which is transmitted, and the upper end of the tolerance range; the second line passes through the same sample and the lower end of the tolerance range.

b. A subsequent sample is redundant and can be discarded when one end of the tolerance range placed around the sample falls within the corridor. The sample itself is not required to be within the corridor. Each redundant sample modifies the corridor extended to the next sample in the following way.

If one of the boundary lines of the corridor does not pass through the tolerance range placed around the redundant sample, a new boundary is established that passes through the nearest end point of the tolerance range.

c. If the tolerance range placed about a sample does not overlap the corridor, the sample is nonredundant, but it is not transmitted. Rather, an artificial value for the preceding sample is transmitted, which is simply the predicted value for the previous sample. This value is the midpoint of the corridor at the time corresponding to the previous sample, and the corridor is the one used for analysis of the nonredundant sample.

Rules for reconstruction are as follows:

a. Transmitted samples are connected by straight lines.

b. The maximum peak error between the raw data and the reconstruction, processed data is plus or minus one-half tolerance range.

These rules are illustrated in Figure 11.

JUPITER DATA REDUNDANCY STUDY

The Jupiter Data Redundancy Study was initiated in 1961. Its purpose was to determine whether redundant information was telemetered in all instances or situations of flight behavior, and if a redundancy removal device would be overwhelmed if a catastrophic condition occurred.

Three flight telemetry recordings were studied: a normal flight, a flight in which abnormal conditions occurred (out-of-tolerance conditions, etc.), and a flight in which the missile was destroyed (i.e., a catastrophic failure).

The analysis revealed that redundant information was contained in the telemetered messages even in the catastrophic flight, and that the entire sensor ensemble feeding the telemetry link did not seem to go so active as to swamp or overwhelm a redundancy removal device.

The results of this study were very encouraging and established the practical advantages of using an airborne redundancy removal device [2].

BREADBOARD DEVELOPMENT OF SIMPLE (ZFN) ALGORITHM DEVICE

The Jupiter Data Redundancy Study led directly to the development of a breadboard implementation of a single algorithm (ZFN). The purpose of the breadboard was to detect some of the problems of implementing an algorithm into redundancy removal flight

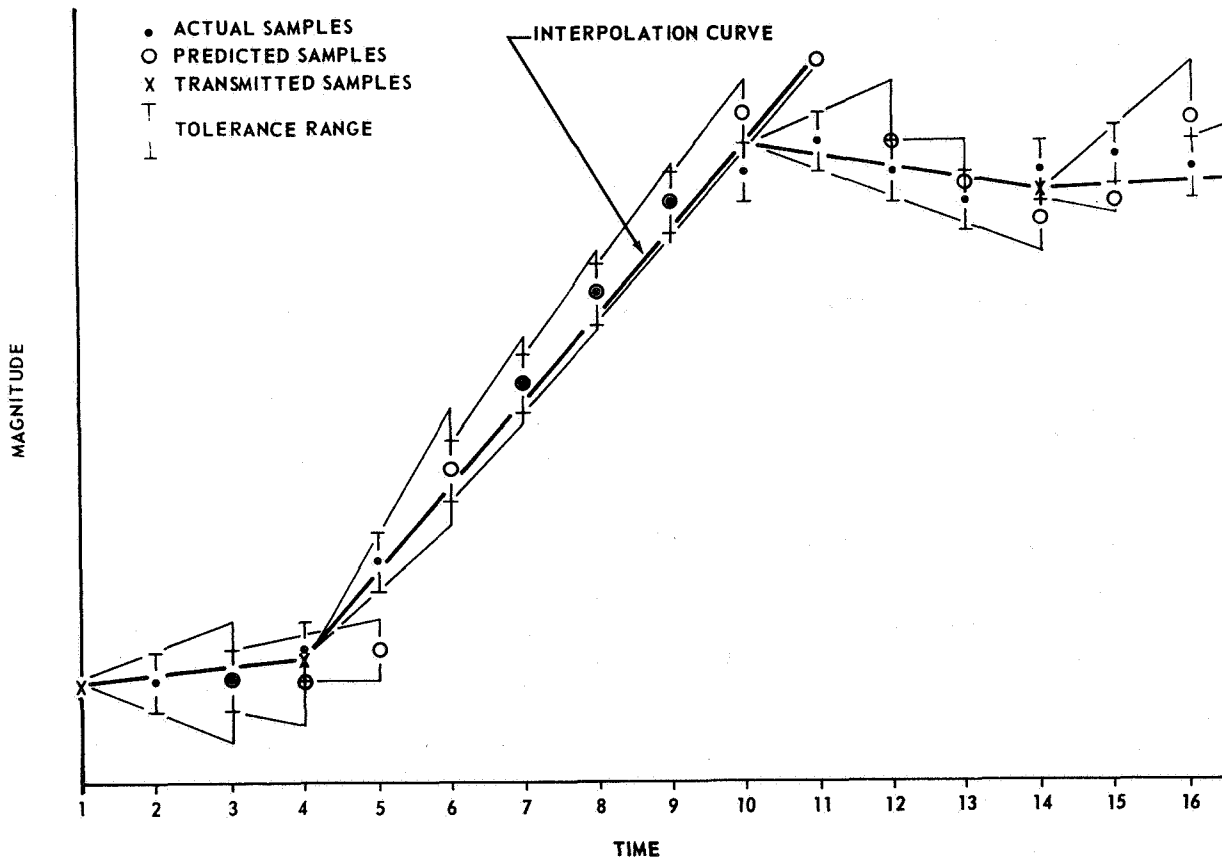


FIGURE 11. FIRST ORDER, VARIABLE CORRIDOR, ARTIFICIAL PRECEDING SAMPLE TRANSMITTED (FVA)

equipment (even if only to the breadboard stage). Although several problems were uncovered and solved in the fabrication and evaluation of the breadboard unit, none of the problems were serious. As a result of developing the breadboard unit, the use of algorithms in airborne redundancy removal flight equipment seemed feasible.

ZFN FLIGHT UNIT DEVELOPMENT AND FABRICATION

Early in 1963, work was begun on the development of redundancy removal flight equipment. The information derived from the development of the breadboard redundancy removal device was used to fabricate the first airborne unit (also of the simple ZFN algorithm type).

Such problems as establishing efficient memory addressing schemes, combining nondestructive read-

out (NDRO) and destructive readout (DRO) memory section, etc., were overcome in the development phase. Since the breadboard unit revealed most of the problem areas, the flight unit was built with a minimum number of problems to overcome.

Specifically, the unit (the telemetry redundancy removal device) was designed to reduce the transmitter bandwidth required for transmission of telemetry data. It was designed to accept PCM data, to examine the input data for significant information, and to provide a compressed PCM (CPCM) output for transmission. All phases of the design were compatible with existing procedures for Saturn flight equipment.

The resulting unit is shown in Figure 12. The block diagram is shown in Figure 13. A complete description of the ZFN redundancy removal unit and its operation is given by Horton and Massey [3]. Basically, the unit has four subsections: the logic

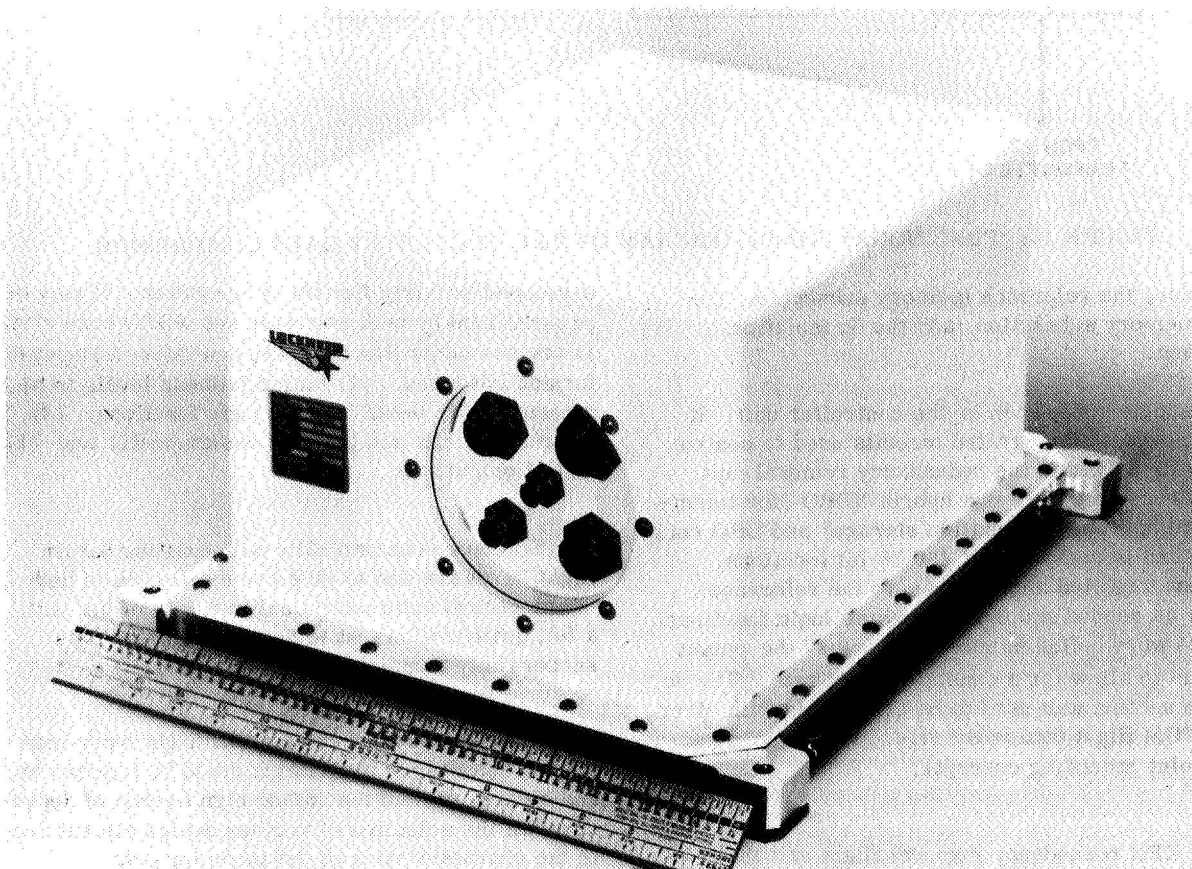


FIGURE 12. ZFN AIRBORNE REDUNDANCY REMOVAL UNIT

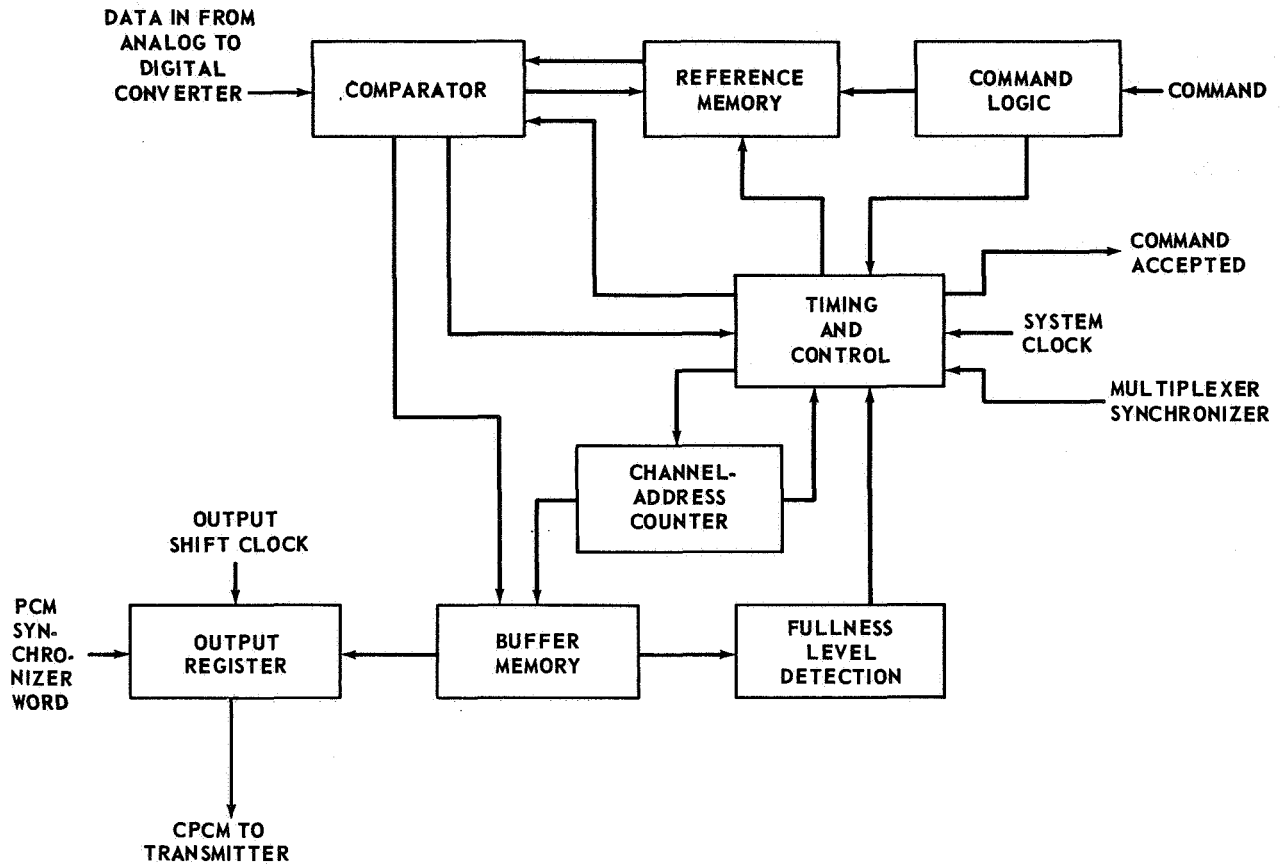


FIGURE 13. FUNCTIONAL BLOCK DIAGRAM OF THE TELEMETRY DATA COMPRESSOR

subsection, the reference memory subsection, the buffer memory subsection, and the dc isolation subsection.

The logic subsection is the controller unit. It contains over 460 integrated circuits used to control the operations within the redundancy removal unit. The reference memory is a hybrid NDRO (for telemetry word address information storage) and DRO combination and is composed of 480 26-bit locations. Words are recalled and returned to the reference memory as needed and dictated by the logic functions. The 1024 word buffer memory "smooths" the output wavetrain to allow for a constant output rate. The dc isolation section was used to be compatible with other Saturn PCM flight equipment (i.e., to maintain the single point grounding concept).

The ZFN redundancy removal flight unit that was

developed is fairly flexible in operation. It may be programmed by both hardware and NDRO core storage to accommodate five different functions: (1) input data format and rates, (2) buffer fullness levels to be detected, (3) detail control logic functions, (4) tolerance limits and priority assignments, and (5) CPCM output rate.

To insure compatibility with existing Saturn flight hardware and to give some measure of both the electrical and mechanical integrity of the unit, a full qualification test to Saturn standards was successfully completed.

Building redundancy removal flight equipment proved that simple algorithms could be implemented and clearly showed the rather high degree of dependency of the selection of various design alternatives to the characteristics of the incoming data.

COMPUTER STUDIES OF REAL AND SIMULATED DATA

As more possibilities of redundancy removal became obvious, a more precisely programmed analytical investigation was organized. In 1963, computer studies were initiated that made use of both real and simulated PCM flight data for input information. The eight algorithms were studied to determine which one would be desirable in a particular situation. Many factors (such as implementation cost, etc.) would have to be considered before an actual system could be designed, but the computer studies were made on a broader basis.

Initially, actual data from Saturn flight S-1 were used in the first computer studies. To determine more of the limitations inherent in using the eight

algorithms, simulated data were also used in the computer studies. At this point, the primary result is outlined in Figure 14. The entire results of the computer studies (both real and simulated data) were well reported in detail by Bjorn, James, Griffin, and Simpson [1].

The results of the initial computer studies (1964) indicated that additional analyses of the eight selected algorithms would be of considerable potential use. Five redundancy removal algorithms were used to study PCM data from SA-7, SA-8, SA-9, and SA-10 Saturn vehicles (three of the original eight were dropped because they afforded the lowest compression ratio for an allowable rms error). The results of these studies show the relative performance of the five algorithms and the effect of the particular flight and type measurement on the redundancy content of

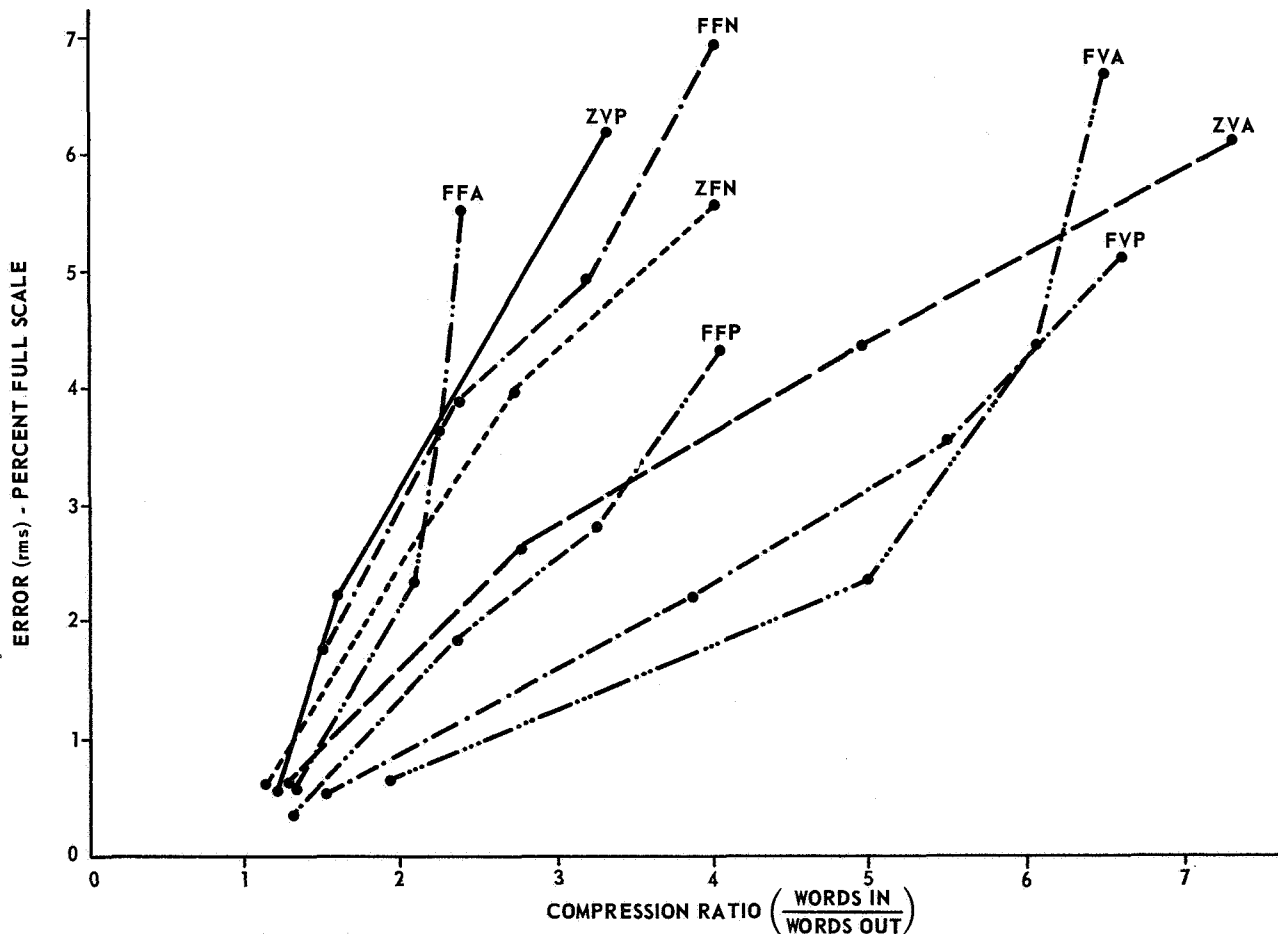


FIGURE 14. ERROR (rms) VERSUS COMPRESSION RATIO FOR THE 5th ORDER DATA (RSR = 10)

the data. Also outlined during these studies was the propensity of several algorithms to "oscillate" or produce data samples because of small data variations relative to the tolerance range explored. Typical graphs of rms error versus compression ratio for the five algorithms are shown in Figures 15 through 22. As in the previous computer studies, the results of these studies were reported in detail by Haskew and Simpson [4].

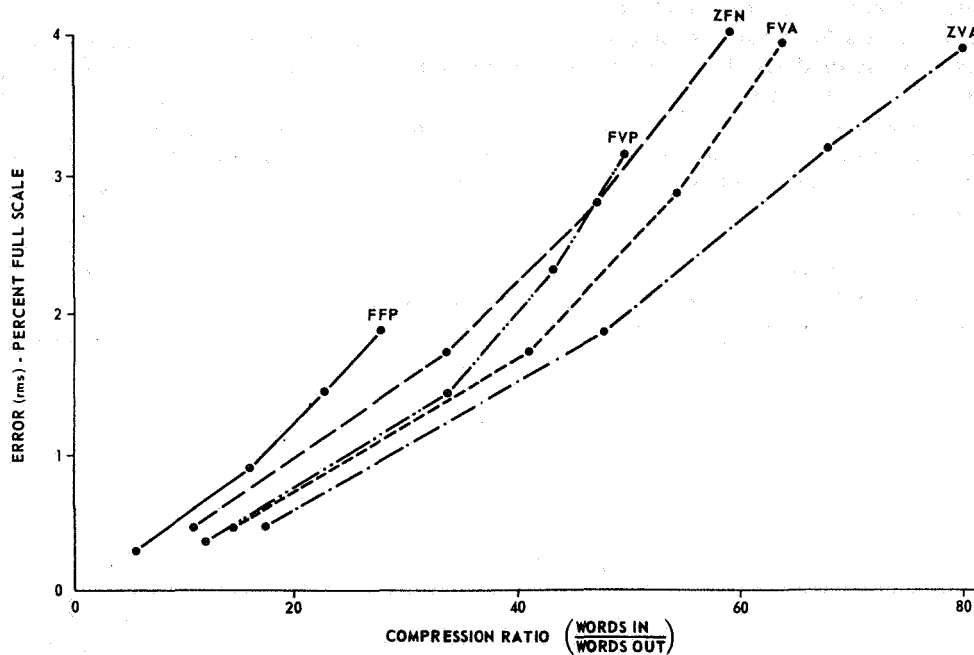


FIGURE 15. ERROR (rms) VERSUS COMPRESSION RATIO FOR SA-7 TEMPERATURE MEASUREMENTS

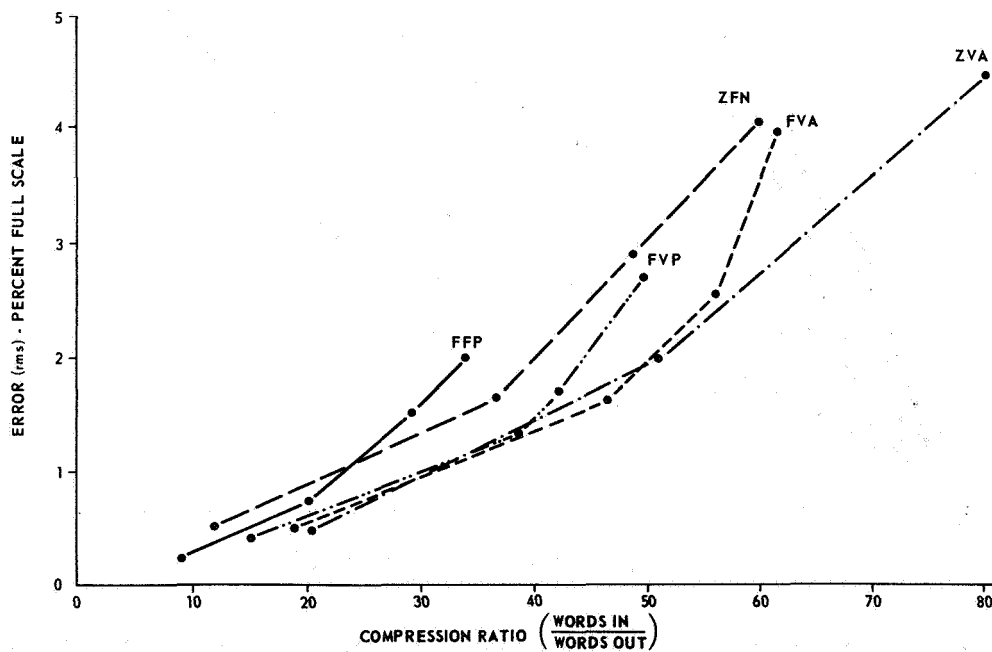


FIGURE 16. ERROR (rms) VERSUS COMPRESSION RATIO FOR SA-8 TEMPERATURE MEASUREMENTS

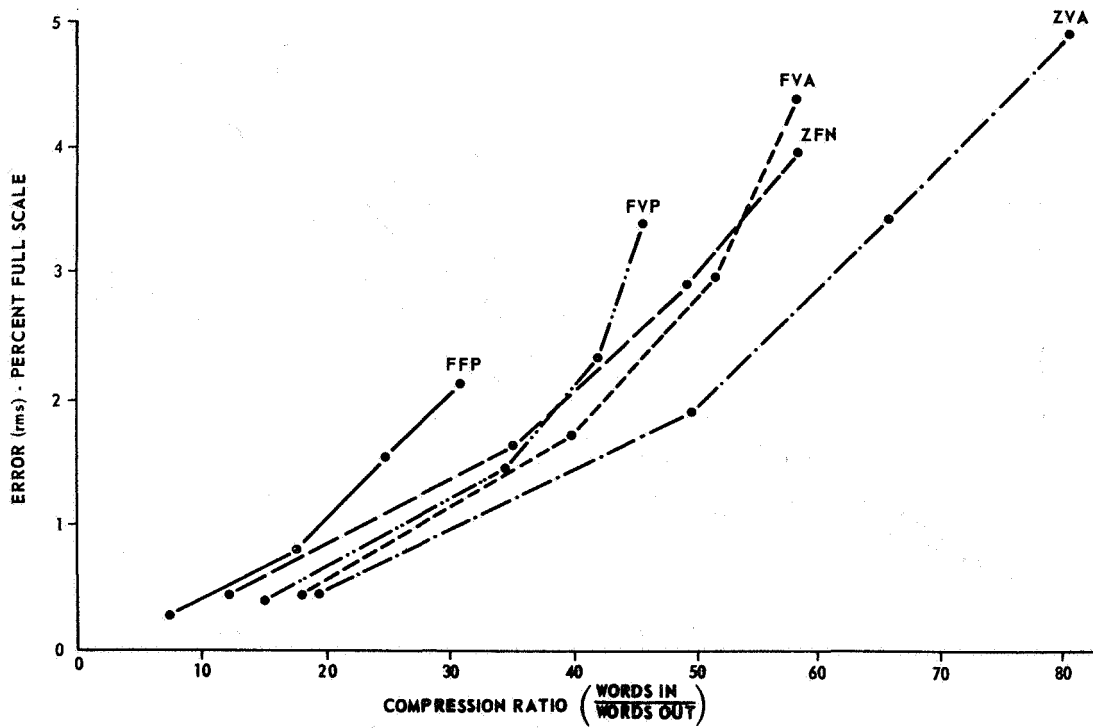


FIGURE 17. ERROR (rms) VERSUS COMPRESSION RATIO FOR SA-9 TEMPERATURE MEASUREMENTS

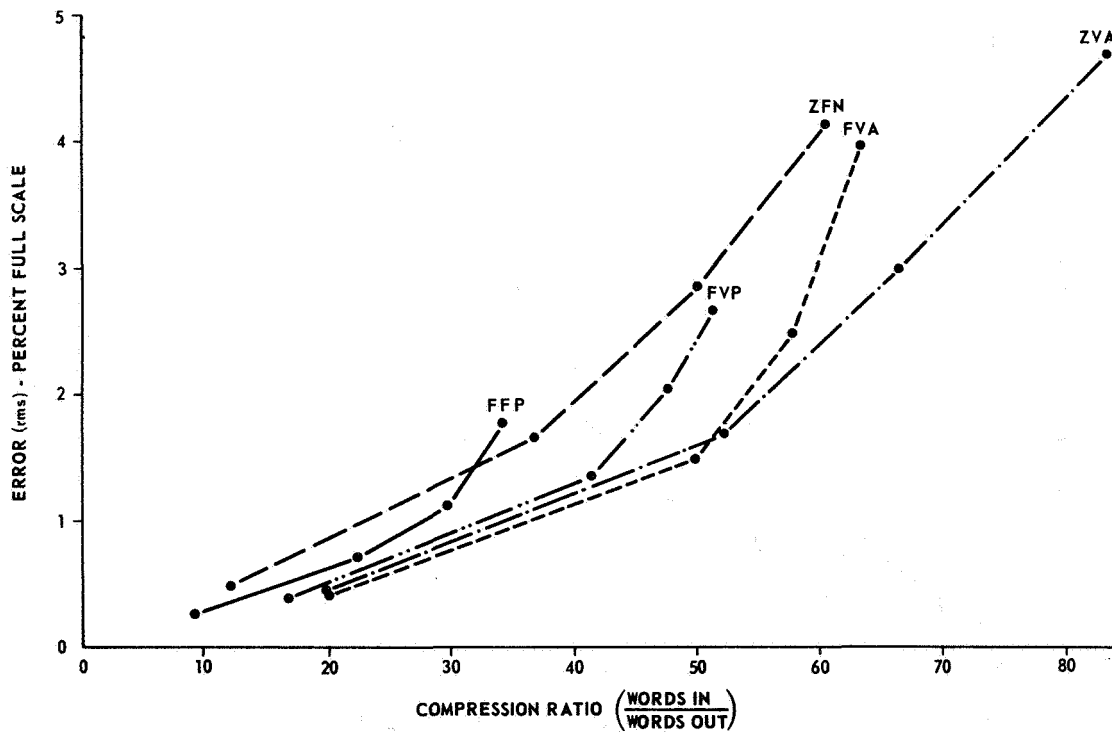


FIGURE 18. ERROR (rms) VERSUS COMPRESSION RATIO FOR SA-10 TEMPERATURE MEASUREMENTS

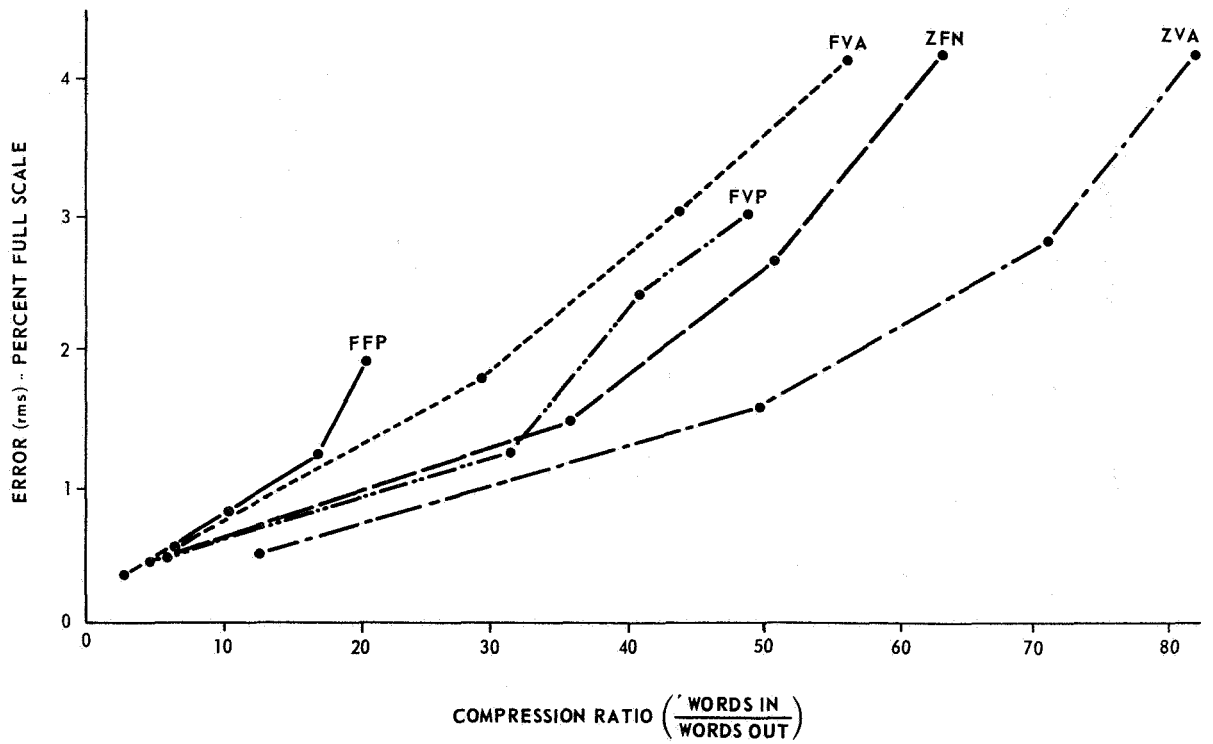


FIGURE 19. ERROR (rms) VERSUS COMPRESSION RATIO FOR SA-7 PRESSURE MEASUREMENTS

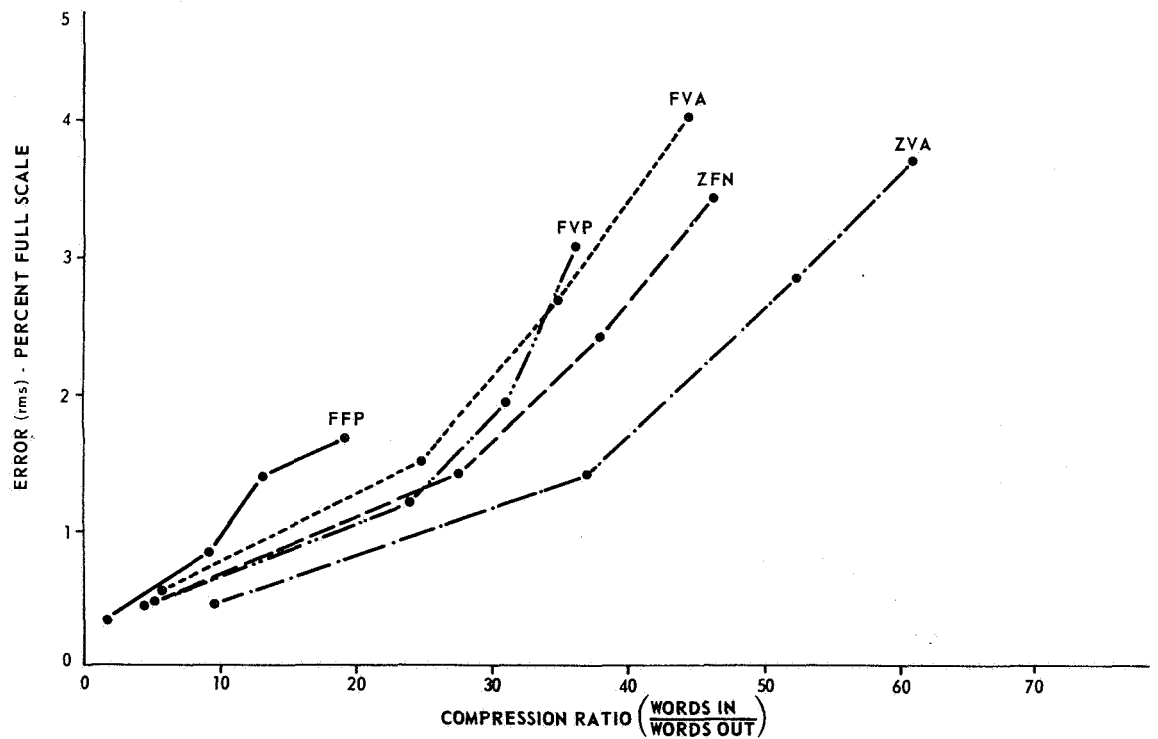


FIGURE 20. ERROR (rms) VERSUS COMPRESSION RATIO FOR SA-8 PRESSURE MEASUREMENTS

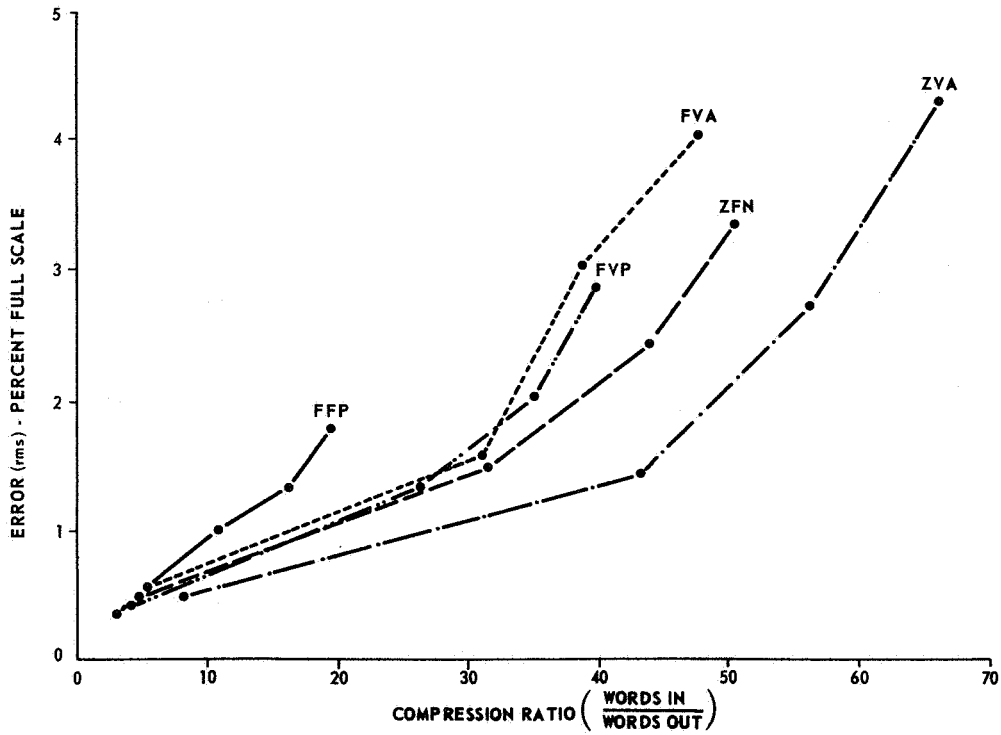


FIGURE 21. ERROR (rms) VERSUS COMPRESSION RATIO FOR SA-9 PRESSURE MEASUREMENTS

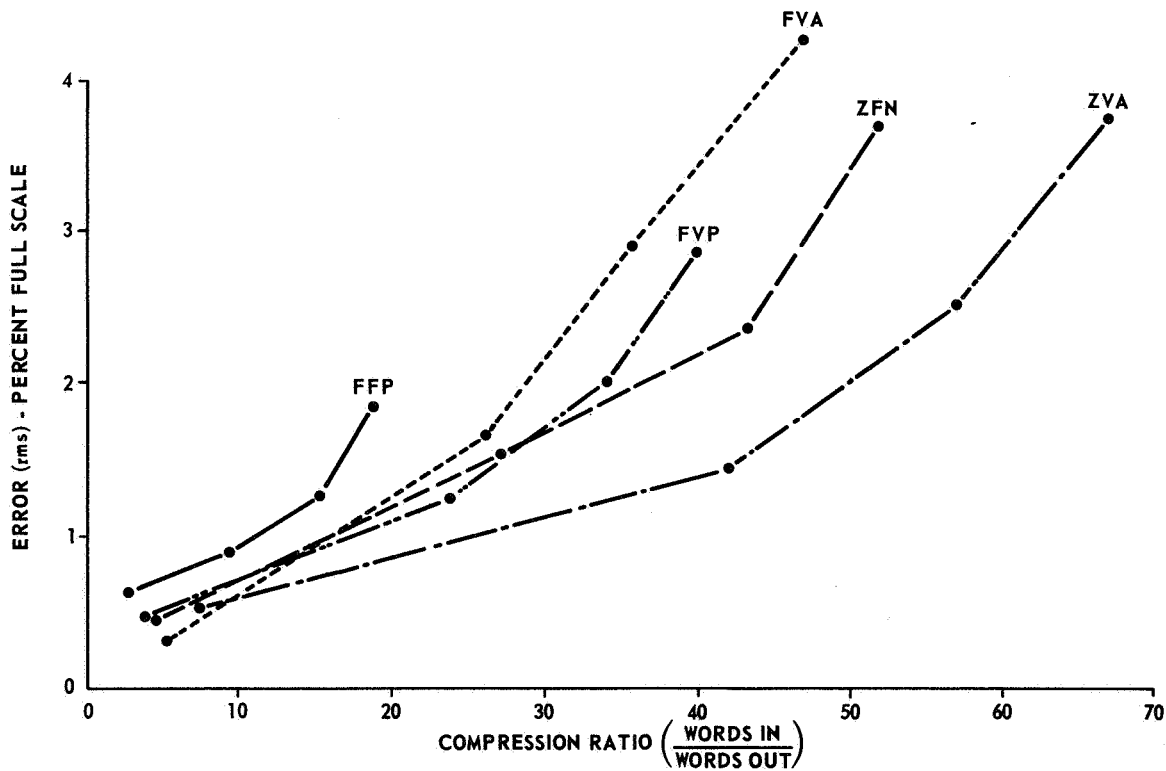


FIGURE 22. ERROR (rms) VERSUS COMPRESSION RATIO FOR SA-10 PRESSURE MEASUREMENTS

RECENT DEVELOPMENTS IN HARDWARE

The development of the first redundancy removal flight unit (ZFN type) and the subsequent computer studies established that data characteristics were important to the resultant "compressibility" of data, and also were important factors in the selection of design alternatives for actual flight hardware implementation. These past occurrences led to two considerations.

The first consideration was that some types of data are easily compressed (i.e., the redundant content reduces without excessive data degradation).

The second consideration was the need to analyze as much data as possible for all five selected algorithms. Thus the telemetry redundancy analyzer (TRA) was developed (Fig. 23). This versatile unit has many capabilities. It basically is a laboratory tool for convenient and economical analysis of large quantities of space vehicle data when using one of the five algorithms (the same five algorithms covered earlier). The analysis can determine the compression ratio and resultant data degradation introduced by using each of the five algorithms on a particular sample of information. This unit can work up to an input rate of 20,000 words/second. In all cases the output is a printed record supplied by a high speed printer located on the front panel. Capabilities of the unit are as follows: the sample time and sample rate may be adjusted from the front panel, a direct D^2/N printout (a mean square error figure) is available, the number of nonredundant samples (NRS) can be printed out, and error distribution can be shown. From these parameters, it is possible to determine undersampling or oversampling and also to find the necessary queue length to process a certain sample with a specific algorithm.

The TRA unit is presently being checked out and data processing is expected to begin in the near future. At least some of the potential results are obvious.

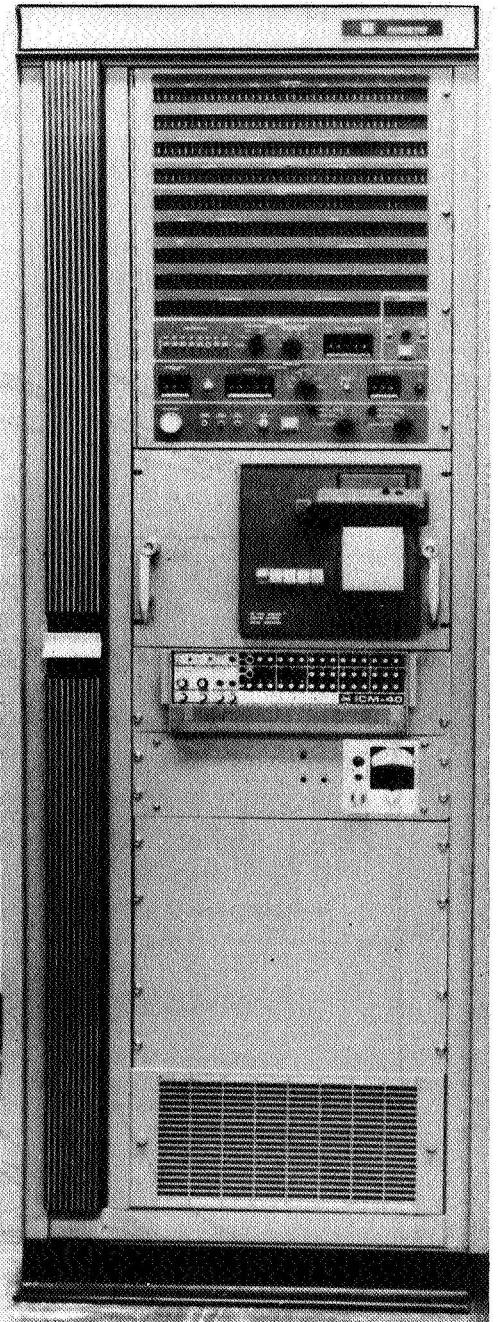


FIGURE 23. TELEMETRY REDUNDANCY ANALYZER

CONCLUSIONS

Previous achievements accomplished by the redundancy removal program are as follows:

1. Jupiter Data Redundancy Study - discovery of significant redundancy content in three Jupiter flights
2. ZFN Breadboard Developed - initial redundancy reduction device implemented
- some implementation problems resolved
3. ZFN Flight Unit Developed - proof that redundancy removal device could be implemented to Saturn flight standards
- acknowledgement of the high degree of dependency of selection of design alternatives on data characteristics
4. Computer Studies of Real and Simulated Flight Data for Determination of Suitability of Different Algorithm/Data Choices - selection of five "promising" ZFN-ZVA-FVA-FVP-FFP
- determination of favorable algorithm (ZVA/FVA) device
- realization of need for lab test unit to conveniently analyze large quantities of space vehicle data

2. Testing of ZVA/FVA

3. ZFN Flight Unit Buffer Fullness Study

- determination if under-sampling or oversampling
- determination of necessary queue length to process a certain sample with a specific algorithm.
- determination of effectivity on Saturn flight data
- determination of suitability for implementation into actual flight equipment.
- determination of best buffer controls
- determination of data compression figures

Projects for the immediate future and the goals to be attained are as follows:

1. Use of Telemetry Redundancy Analyzer - investigation of photo imaging type data
- investigation of Saturn PCM/FM flight data
2. Development of Future Redundancy Removal Units - more efficient telemetry systems accompanying benefits in BW reduction, etc.

REFERENCES

1. Bjorn, T. ; James, S. N. ; Griffin, M. A. ; and Simpson, R. S. : A Study of Redundancy Removal for Saturn Telemetry Data. University of Alabama, Bureau of Engineering Research, Technical Report No. 5, MSFC Contract NAS8-5003, November 1964.
2. Weber and Wynhoff: The Concept of Self Adaptive Data Compression. Packard Bell, PGSET Record, October 1962.
3. Horton, J. A. ; and Massey, H. N. : Advanced Telemetry System with Adaptive Capability.

Present projects and the expected accomplishments are as follows:

1. Development of Telemetry Redundancy Analyzer (For Flight Data) - determination of compression ratio and resultant data degradation when employing one of five different algorithms.
- determination of D^2/N (mean square error figure)
- error distribution with various algorithms

- Lockheed Missiles and Space Corporation,
LMSC 8-39-65-4, MSFC Contract NAS8-5110,
November 1, 1965.
4. Haskew, J. R. ; and Simpson, R. S. : A Study of Redundancy in Saturn Flight Data. University of Alabama, Bureau of Engineering Research, Technical Report No. 9, MSFC Contract NAS8-20172, August 1966.
 4. Horton, J. A. ; Massey, H. N. ; and Smith, W. E. : Advanced Telemetry System With Adaptive Capability. Lockheed, Report LMSC 657617, Annual Technical Report, MSFC Contract NAS8-5110, July 10, 1963.
 5. Horton, J. A. ; and Massey, H. N. : Advanced Telemetry System With Adaptive Capability. Lockheed, LMSC 8-39-65-4, MSFC Contract NAS8-5110, November 1, 1965.
 1. Alylsworth, R. ; Bischoff, R. ; Knight, G. R. ; Medlin, J. E. ; Saffir, O. S. ; Schomburg, R. A. ; Weber, D. R. ; and Hulme, J. R. : Techniques and Application of Data Compression. Lockheed Missiles and Space Company, LMSC 8-51-63-2, June 1963.
 2. Bjorn, T. ; James, S. N. ; Griffin, M. A. ; and Simpson, R. S. : A Study of Redundancy Removal for Saturn Telemetry Data. University of Alabama, Bureau of Engineering Research, Technical Report No. 5, MSFC Contract NAS8-5003, November 1964.
 3. Haskew, R. J. ; and Simpson, R. S. : A Study of Redundancy in Saturn Flight Data. University of Alabama, Bureau of Engineering Research, Technical Report No. 9, MSFC Contract NAS8-20172, August 1966.
 6. James, S. N. ; and Simpson, R. S. : Compressibility of Saturn S-I PCM Data. University of Alabama, Bureau of Engineering Research, Technical Report No. 1, MSFC Contract NAS8-5003, June 1963.
 7. Packard Bell Computer: Redundancy Data Analysis Study Report. Final Technical Report MSFC Contract NAS8-1641, Report No. PBC-4121, March 1962.
 8. Weber; and Wynhoff: The Concept of Self Adaptive Data Compression, Packard Bell, PGSET Record, October 1962.

BIBLIOGRAPHY

APPROVAL

RESEARCH ACHIEVEMENTS REVIEW
VOLUME III REPORT NO. 1

The information in these reports has been reviewed for security classification. Review of any information concerning Department of Defense or Atomic Energy Commission programs has been made by the MSFC Security Classification Officer. These reports, in their entirety, have been determined to be unclassified.

These reports have also been reviewed and approved for technical accuracy.



W. HAEUSSERMANN
Director, Astrionics Laboratory

UNITS OF MEASURE

In a prepared statement presented on August 5, 1965, to the U. S. House of Representatives Science and Astronautics Committee (chaired by George P. Miller of California), the position of the National Aeronautics and Space Administration on Units of Measure was stated by Dr. Alfred J. Eggers, Deputy Associate Administrator, Office of Advanced Research and Technology:

"In January of this year NASA directed that the international system of units should be considered the preferred system of units, and should be employed by the research centers as the primary system in all reports and publications of a technical nature, except where such use would reduce the usefulness of the report to the primary recipients. During the conversion period the use of customary units in parentheses following the SI units is permissible, but the parenthetical usage of conventional units will be discontinued as soon as it is judged that the normal users of the reports would not be particularly inconvenienced by the exclusive use of SI units."

The International System of Units (SI Units) has been adopted by the U. S. National Bureau of Standards (see NBS Technical News Bulletin, Vol. 48, No. 4, April 1964).

The International System of Units is defined in NASA SP-7012, "The International System of Units, Physical Constants, and Conversion Factors," which is available from the U. S. Government Printing Office, Washington, D. C. 20402.

SI Units are used preferentially in this series of research reports in accordance with NASA policy and following the practice of the National Bureau of Standards.

CALENDAR OF REVIEWS

FIRST SERIES (VOLUME I)

<u>REVIEW</u>	<u>DATE</u>	<u>RESEARCH AREA</u>	<u>REVIEW</u>	<u>DATE</u>	<u>RESEARCH AREA</u>
1	2/25/65	RADIATION PHYSICS	12	9/16/65	AERODYNAMICS
2	2/25/65	THERMOPHYSICS	13	9/30/65	INSTRUMENTATION
3	3/25/65	CRYOGENIC TECHNOLOGY	14	9/30/65	POWER SYSTEMS
4*	3/25/65	CHEMICAL PROPULSION	15	10/28/65	GUIDANCE CONCEPTS
5	4/29/65	ELECTRONICS	16	10/28/65	ASTRODYNAMICS
6	4/29/65	CONTROL SYSTEMS	17	1/27/66	ADVANCED TRACKING SYSTEMS
7	5/27/65	MATERIALS	18	1/27/66	COMMUNICATIONS SYSTEMS
8	5/27/65	MANUFACTURING	19	1/6/66	STRUCTURES
9	6/24/65	GROUND TESTING	20	1/6/66	MATHEMATICS AND COMPUTATION
10	6/24/65	QUALITY ASSURANCE AND CHECKOUT	21	2/24/66	ADVANCED PROPULSION
11	9/16/65	TERRESTRIAL AND SPACE ENVIRONMENT	22	2/24/66	LUNAR AND METEOROID PHYSICS

SECOND SERIES (VOLUME II)

<u>REVIEW</u>	<u>DATE</u>	<u>RESEARCH AREA</u>	<u>REVIEW</u>	<u>DATE</u>	<u>RESEARCH AREA</u>
1	3/31/66	RADIATION PHYSICS	7	3/30/67	CRYOGENIC TECHNOLOGY
2	3/31/66	THERMOPHYSICS	8**	5/25/67	COMPUTATION
3	5/28/66	ELECTRONICS	9	7/27/67	POWER SYSTEMS
4	7/28/66	MATERIALS	10	9/28/67	TERRESTRIAL AND SPACE ENVIRONMENT
5	9/29/66	QUALITY AND RELIABILITY ASSURANCE	11	11/30/67	MANUFACTURING
6	1/26/67	CHEMICAL PROPULSION	12	1/25/68	INSTRUMENTATION RESEARCH FOR GROUND TESTING

THIRD SERIES (VOLUME III)

<u>REVIEW</u>	<u>DATE</u>	<u>RESEARCH AREA</u>	<u>REVIEW</u>	<u>DATE</u>	<u>RESEARCH AREA</u>
1	3/28/68	AIRBORNE INSTRUMENTATION AND DATA TRANSMISSION	3	7/25/68	CONTROL SYSTEMS
2	5/22/68	ASTRODYNAMICS, GUIDANCE AND OPTIMIZATION	4	9/26/68	AEROPHYSICS

* Classified. Proceedings not published.

** Proceedings summarized only.

Correspondence concerning the Research Achievements Review Series should be addressed to:
Chief, Research Program Office, R-EO-R, Marshall Space Flight Center, Alabama 35812